Spatio-temporal dynamics and biogeochemical properties of green seawater discolorations caused by the marine dinoflagellate *Lepidodinium chlorophorum* along southern Brittany coast

Pauline Roux [a], Raffaele Siano [b], Philippe Souchu [a], Karine Collin [a], Anne Schmitt [a], Soazig Manach [a], Michael Retho [c], Olivier Pierre-Duplessix [a], Laetitia Marchand [c], Sylvia Colliec-Jouault [c], Victor Pochic [d], Maria Laura Zoffoli [d], Pierre Gernez [d], Mathilde Schapira [a],*

[a] *Ifremer, LITTORAL, F-44300, Nantes, France*
[b] *Ifremer, DYNECO, F-29280, Plouzané, France*
[c] *Ifremer, BRM, F-44300, Nantes, France*
[d] *Nantes Université, Institut des Substances et Organismes de la Mer, ISOMer, UR 2160, F-44000, Nantes, France*

ARTICLE INFO

ABSTRACT

Blooms of the marine dinoflagellate *Lepidodinium chlorophorum* cause green seawater discolorations affecting the recreational use and the tourism economy along southern Brittany (NE-Atlantic, France). Hypoxic conditions associated with phytoplankton biomass recycling are suspected to cause fauna mortalities. An *in situ* monitoring was performed in 2019 to characterise the seasonal variability of *L. chlorophorum*. This species was observed from May to November, with a maximum abundance in June–July. Specific bloom sampling demonstrated a dominance of *L. chlorophorum* within microphytoplankton, and documented its vertical distribution. Satellite observation was used to compute the surface extent of the bloom and to highlight the importance of small-scale temporal variability, with tidal currents being a primary driver of surface distribution of the bloom. Stratification contributed to promoting the bloom of *L. chlorophorum*. High concentrations of phosphate and ammonium, together with transparent exopolymer particles (TEP), were recorded within the bloom. Bacterial stimulation, leading to nutrient remineralisation or mucus facilitating mixotrophy, is suggested to sustain bloom development. Hence, TEP production might provide an ecological advantage for the dinoflagellate, conversely causing negative effects on the environment and biological resources through hypoxia. These first insights constitute a baseline for further studies in other ecosystems impacted by this species.

1. Introduction

Phytoplankton blooms in marine coastal ecosystems can lead to the accumulation of a high biomass of photosynthetic microorganisms (protists and cyanobacteria; Cloern, 1996). These accumulations often occur at the land-sea interface when the cellular positive net growth surpasses biomass losses, resulting from the interplay of biological and physical environmental parameters. In coastal systems, phytoplankton blooms are controlled by physico-chemical factors, such as inputs from river flow (Peierls et al., 2012; Hall et al., 2013), coastal upwelling (Brown and Ozretich, 2009), atmospheric deposition (Paerl, 1997), wind (Iverson et al., 1974; Carstensen et al., 2005), nutrient availability (Margalef, 1978), tidal mixing and stratification (Cloern, 1996), heat waves that set up thermal stratification (Cloern et al., 2005), increasing residence time of water (Odebrecht et al., 2015), seasonal changes in temperature, and solar irradiance (Shikata et al., 2008), and biological variables, such as benthic and planktonic grazing pressure (Carstensen et al., 2007; Cloern et al., 2007; Petersen et al., 2008), parasites (Siano et al., 2011; Garvetto et al., 2018), and viral infections (Suttle, 2007).

When occurring at a high biomass, these natural phenomena may cause surface seawater discoloration (i.e., green, red, brown) and/or foam production, thus altering the appearance of coastal waters (Siano et al., 2020) and can have significant impacts on ecosystem functions and services. By altering the aesthetic quality of the coastal areas,

seawater discolorations have a negative effect on tourism (Zingone and Enevoldsen, 2000), and the remineralisation of the high volume of biomass produced during intense blooms may create hypoxic/anoxic conditions that are deleterious for marine aquaculture (Sournia et al., 1992). The increase in the distribution and severity of these events may be driven by climate change (Hallegraeff, 2010; Gobler et al., 2017). However, a better understanding of the dynamics and consequences of water discolorations in coastal areas is still needed.

Seawater discoloration in marine coastal waters is produced by different photosynthetic protists and cyanobacteria. Depending on phytoplankton abundances and light intensity, different shades of red discolorations may be induced by the development of various dinoflagellates (e.g., *Noctiluca scintillans*; Quevedo et al., 1999; Cabal et al., 2008; Zhang et al., 2020) and ciliates (e.g., *Mesodinium rubrum*; Zhang et al., 2020). While dark brown discolorations caused by diatoms are frequently reported worldwide, other phytoplankton species of the phylum Ochrophyta (Heterokontophyta) could also be responsible for dark brown discolorations, including members of the class Raphidophyta and Dictyochophyta (Siano et al., 2020). Green-pigmented microalgal classes (Prasinophyta and Cyanophyta) are known to frequently cause green blooms. The capacity of the marine dinoflagellate *Lepidodinium chlorophorum* to form green seawater discoloration is due to the presence of a green plastid containing chlorophyll *b* (Matsumoto et al., 2011) inherited from a secondary endosymbiosis with a chlorophyte (Kamikawa et al., 2015; Gavalás-Olea et al., 2016; Jackson et al., 2018). Blooms of this unarmoured dinoflagellate (Elbrächter and Schnepf, 1996; Hansen et al., 2007) have been observed in coastal waters worldwide, including Chile (Iriarte et al., 2005; Rodríguez-Benito et al., 2020), California, USA (Gárate-Lizárraga et al., 2014), Australia (McCarthy, 2013), and Europe (Honsell and Talarico, 2004; Sourisseau et al., 2016). Green seawater discolorations due to the massive development of *L. chlorophorum* have been frequently reported in southern Brittany since 1982 (Sournia et al., 1992; Siano et al., 2020).

Although the occurrence of *L. chlorophorum* is relatively well documented (Honsell et al., 1988; Sournia et al., 1992; Paulmier et al., 1995; Elbrächter and Schnepf, 1996; Sourisseau et al., 2016; Karasiewicz et al., 2020; Siano et al., 2020; Serre-Fredj et al., 2021), the biological and ecological properties that make this species successful in the environment have not yet been fully elucidated. Blooms of this dinoflagellate, which are mainly observed during summer (Belin et al., 2021; Siano et al., 2020), could be supported by the recycling of organic nitrogen in its ammonium form (Sourisseau et al., 2016). This eurythermal and euryhaline dinoflagellate (Elbrächter and Schnepf, 1996; Claquin et al., 2008) has been observed in river plumes (Sournia et al., 1992; Sourisseau et al., 2016), and the highest densities have been reported occasionally at the pycnocline in stratified waters (Sourisseau et al., 2016). In 2010, high densities of this species ($>10^6$ cells L^{-1}) were observed across the Loire River plume (Sourisseau et al., 2016). Furthermore, several studies suggested that *L. chlorophorum* could be considered mixotrophic (Hansen and Moestrup, 2005; Jeong et al., 2010; Sourisseau et al., 2016; Ng et al., 2017). The mixotrophic or pure autotrophic characteristic may have strong implications for understanding bloom dynamics. However, while a strain of *Lepidodinium* sp., isolated recently from subtropical coastal waters, has been shown to be a facultative mixotroph (Liu et al., 2021), to our knowledge, the mixotrophy by *L. chlorophorum* off Brittany has not yet been clearly established. Moreover, the life cycle of *L. chlorophorum* has rarely been studied so far. Benthic cyst production has not been observed, and despite some observations in culture (Sournia et al., 1992), the existence of temporary cysts in the field remains unclear.

Lepidodinium chlorophorum is not known to produce toxigenic substances for human or marine fauna, but under non-limiting culture conditions, it excretes a large amount of transparent exopolymer particles (TEP; Claquin et al., 2008; Roux et al., 2021) which may impact marine fauna. TEP are composed of a large amount of carbon, and their aggregations tend to accelerate organic matter sedimentation (Passow

et al., 2001; Mari et al., 2017; Bittar et al., 2018). Blooms of *L. chlorophorum* have been associated with mass mortalities of fish and cultivated bivalves along the Atlantic French coast (Sournia et al., 1992; Chapelle et al., 1994; Siano et al., 2020), and numerical models have suggested that oysters (*i.e. Crassostrea gigas*) may be negatively affected when feeding upon *L. chlorophorum* (Alunno-Bruscia et al., 2011; Thomas et al., 2016). Even though the direct effect of TEP produced by *L. chlorophorum* on marine fauna remains to be elucidated, post-bloom hypoxic/anoxic conditions associated with the recycling of high biomass (phytoplankton cells and TEP) are suspected to be a major cause of fauna mortalities (Sournia et al., 1992; Siano et al., 2020). However, to our knowledge, no study has investigated whether the high production of TEP *in situ* may provide a negative impact and/or an ecological advantage for *L. chlorophorum*.

This study aimed to describe seasonal variation of *L. chlorophorum* as well as to document bloom biogeochemical properties in the Vilaine Bay (NE Atlantic, France), a coastal area regularly impacted by eutrophication and subsequent algal proliferation (Ratmaya et al., 2019). A specific monitoring field campaign was performed in 2019 to characterise the seasonal variation of this species. To further investigate green seawater discoloration dynamics, high-resolution satellite data were combined with *in situ* sampling during a bloom event in July 2019. The concentration and composition of extracellular polymeric substances produced during *L. chlorophorum* bloom were characterised and compared with a recent culture study (Roux et al., 2021). Finally, the potential contribution of TEP produced by *L. chlorophorum* on the organic carbon pool was investigated to further assess the potential effects of this biological property of *L. chlorophorum* on ecosystem functioning.

2. Materials and methods

2.1. Study area

South Brittany has been identified as a hot spot for *L. chlorophorum* bloom development in France (Belin et al., 2021), therefore abundance was analysed in two bays of this coast: Quiberon and Vilaine (Fig. 1). These bays were selected based on the recurrent observations of this species within the phytoplankton community (Belin et al., 2021; Siano et al., 2020).

Quiberon Bay is a shallow bay (15 m) characterised by weak tidal currents and receive indirect freshwater inputs, as the Loire and Vilaine River plumes tend to spread toward the NW and remain confined along the coast, particularly during early spring (Lazure and Jégou, 1998). Low freshwater inputs combined with low vertical mixing cause strong haline stratification in this bay (Planque et al., 2004). From spring to mid-September, thermal stratification is superimposed onto the haline stratification. During thermal stratification, W/NW winds may induce local upwelling (Lazure and Jégou, 1998; Puillat et al., 2004, 2006).

Vilaine Bay is a 69 km^2 shallow bay (10 m) directly influenced by the Vilaine and Loire Rivers, with a mean annual flow of 70 and 850 m^3 s^{-1}, respectively (Lazure et al., 2009). The Loire River plume generally spreads NW with a dilution of 20- to 100-fold by the time it reaches the Vilaine (Ménesguen and Dussauze, 2015; Ménesguen et al., 2018). The Vilaine River plume generally spreads throughout the bay before moving westward (Chapelle et al., 1994). A dam located 8 km from the mouth regulate freshwater discharge and was constructed in 1970 to prevent saltwater intrusion upstream (Traini et al., 2015). The Vilaine Estuary is the most sheltered estuary of the French Atlantic coast; the water residence time in the bay varies from 10 to 20 days depending on the season and is generally longer during calm periods (Chapelle et al., 1994). The water circulation is characterized by low tidal and residual currents and is mainly driven by tide, wind, and river flow (Lazure and Salomon, 1991; Lazure and Jégou, 1998). Haline stratification is strong from February to June in response to high river runoff and relatively low vertical mixing, whereas thermal stratification occurs between May and mid-September (Puillat et al., 2004). The Vilaine Bay has undergone
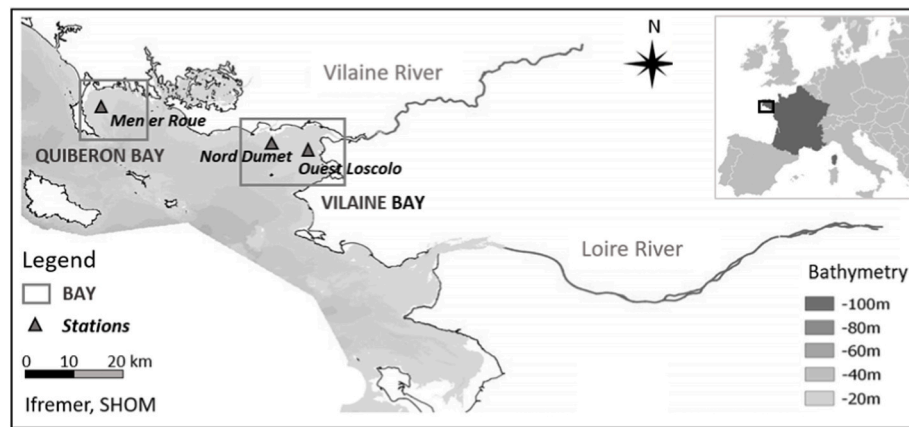
Fig. 1. Location of the three sampling stations of the Vilaine Bay (Nord Dumet, Ouest Loscolo) and Quiberon Bay (Men er Roue) monitored in 2019 in Southern Brittany coast (NE Atlantic, France).

eutrophication for several decades mainly due to the high nutrient inputs from the Vilaine and Loire Rivers (Rossignol-Strick, 1985; Ratmaya et al., 2019).

2.2. Seasonal monitoring in 2019

To determine the timing for *L. chlorophorum* bloom occurrence, monitoring was performed in Quiberon and Vilaine bays from May to December 2019. Sampling was conducted fortnightly at different day times, but according to high tide (± 2 h), at three stations: Men er Roue (Quiberon Bay), Ouest Loscolo, and Nord Dumet (Vilaine Bay; Fig. 1). Vertical profiles of seawater temperature (°C), salinity, turbidity (nephelometric turbidity unit; NTU), and *in vivo* fluorescence (fluorescein fluorescence unit; FFU) were performed with a multi-parameter probe (NKE MP6) from the subsurface to the water-sediment interface (8–14 m, depending on stations). Water samples were collected using a 5 L Niskin bottle at three depths: subsurface (0–1 m), 1 m above the water-sediment interface and at the fluorescence maximum (Fmax) when present. Water sample aliquots were processed for microphytoplankton identification and enumeration and for chlorophyll *a* concentration ([Chl*a*]; µg L^{-1}). Dissolved inorganic nitrogen, phosphorus and silicates concentration ([DIN, DIP, DSi]; µM) were measured as well as TEP ([TEP]; µg Xeq L^{-1}) and particulate organic carbon concentration ([POC]; µM). Analytical procedures are described in section 2.4. At the Nord Dumet station, these data were collected every fortnight, in addition to temperature, salinity, and dissolved oxygen concentrations, which were acquired continuously and autonomously by the MOLIT buoy of the COAST-HF network (Coastal OceAn observing SysTem-High Frequency). This instrumented buoy measured these parameters in 1-h intervals at the subsurface and 1 m above the water-sediment interface (Retho et al., 2020). Data on the river flow was extracted from the French hydrologic database (http://www.hydro.eauf rance.fr/). Daily wind data were retrieved from the weather station Belle Ile – Le Talus (47°17′39″N; 3°13′05″O) from the Météo-France observation network (https://donneespubliques.meteofrance.fr/).

2.3. Specific bloom sampling in summer 2019

On July 9, 2019, a specific sampling strategy was implemented to investigate the spatial structure and hydrological changes caused by the massive development of *L. chlorophorum*. Along a seaward transect, six stations were sampled at high tide: three stations inside and three stations outside the green seawater discoloration. Sampling was performed as previously described. To further investigate the organic matter produced during a bloom, several additional parameters were measured: concentrations of dissolved organic carbon ([DOC]; µM) and nitrogen

([DON]; µM), and nitrite concentration ([NO$_2$]; µM). Moreover, to investigate the composition of the soluble fraction of the extracellular polymeric substances (soluble extracellular polymers, SEP) present within a bloom of *L. chlorophorum*, a subsurface water sample was collected at St1. To complete the characterisation of this bloom event, satellite data were used to estimate its extent and duration.

2.4. Analytical procedure of physicochemical and biological variables

For inorganic nutrients, 300 mL water samples were pre-filtered through 41 µm pore silk directly from the Niskin bottle. For dissolved silicate (i.e., $DSi = Si(OH)_4^-$) concentrations, water samples were filtered through 0.45 µm acetate cellulose membrane and stored at 4 °C until analysis. Water samples for the determination of dissolved inorganic nitrogen (i.e., $DIN = NO_3^- + NO_2^- + NH_4^+$) and phosphorus (i.e., $DIP = PO_4^{3-}$) were stored directly at −20 °C. Samples were analysed using an auto-analyser (Seal analytical AA3) following standard protocols (Aminot and Kérouel, 2007). The limits of quantification (LQ) were 0.4 µM for DSi, 0.5 µM for $NO_3^- + NO_2^-$, and 0.05 µM for DIP NH_4^+, and NO_2^-. Measurement uncertainty measurement was 12% for DSi, 10% for $NO_3^- + NO_2^-$, 15% for DIP, and 27% for NH_4^+.

Total dissolved nitrogen concentrations ([TDN]) was measured using the persulphate oxidation method (Raimbault et al., 1999; Aminot and Kérouel, 2004) and then analysed in segmented continuous flow on the auto-analyser according to Aminot and Kérouel (2007). [DON] were calculated by the difference between [TDN] and [DIN].

To estimate [POC] in the bloom, 100–250 mL were gently filtered onto combusted GF/F filters (Whatman® Nuclepore™; for 4 h at 450 °C) and stored at −20 °C until analysis. After removal of carbonates with phosphoric acid, filters were treated using a CHN element analyser (Thermo Fisher Scientific, Waltham, USA) to measure [POC] and nitrogen ([PON]) concentrations (Aminot and Kérouel, 2004). [DOC] were measured on the filtrates collected in acid washed and pre-combusted glass tubes and stored at −20 °C. Analyses were conducted using a TOC meter (Shimadzu TOC-V$_{CSH}$). Measurement uncertainty was 12%.

The extracellular polymeric substances were analysed to: 1) estimate [TEP] in the bloom and 2) characterise the composition of SEP present within a bloom of *L. chlorophorum*. [TEP] was determined using a semi-quantitative method based on the colorimetric determination of the amount of dye complexed with extracellular particles (Claquin et al., 2008, adapted from Passow and Allldredge, 1995) as described in Roux et al. (2021). Briefly, triplicate samples of 50–150 mL were gently filtered through 0.4 µm polycarbonate membrane filters (Whatman® Nuclepore™ Track-Etched Membrane). Particles retained on the filter were stained with Alcian Blue (Sigma) solution. The filters were soaked

in 80% sulphuric acid for 2 h and absorbance read at 787 nm using a spectrophotometer (Shimadzu UV-2600). The TEP concentrations are expressed in µg xanthan equiv L^{-1}. To characterise the SEP present within a bloom of *L. chlorophorum*, 1 L of subsurface water sample collected at St1, located inside the bloom, was centrifuged (4000 g for 30 min at 4 °C), and protein and monosaccharide contents were characterised (Roux et al., 2021). To confirm the presence of a sulphated polysaccharide, SEP were analysed by both electrophoresis analysis (PAGE gel) and ATR-FTIR spectroscopy and compared to sulphated polysaccharide standards (galactan sulphate MW 80,000, 7.7% S extracted from *Asparagopsis armata*; dextran sulphate sodium salt MW 50,000, 16.0–19.0% S from Sigma D-8787; dextran sulphate sodium salt MW 500,000, 16.0–19.0% S from Sigma D-6001). The PAGE gel (10% w/v acrylamide) was prepared in 1.5 M Tris HCl buffer at pH 8.8 containing ammonium persulphate (0.05% w/v) and tetramethylethylenediamine (Temed). Polyacrylamide stacking gel (4% w/v acrylamide) was prepared in 0.5 M Tris HCl at pH 6.8, ammonium persulphate (10% w/v), and Temed. Samples (40 µL) were prepared in loading buffer (0.5 M Tris HCl pH 6.8, glycerol, 0.5 M EDTA, 0.5% w/v bromophenol) and then loaded on polymerised acrylamide gels. The gel was fixed for 30 min in 12.5% (w/v) trichloroacetic acid and stained for 15 min with toluidine blue (triméthylthionine hydrochloride) solution at 1% (w/v acetone 80%) and then bleached for 2 h with acetic acid 1%. The FT-IR spectra of the sample and standards were recorded at room temperature using OPUS software at the absorbance mode from 4000 to 400 cm^{-1} (100 scans) with a resolution of 4 cm^{-1} using a Golden Gate single reflection diamond ATR system in a Brucker IFS-55 spectrometer.

Phytoplankton biomass was estimated through [Chl*a*]. Water samples (500–1000 mL) were filtered through GF/F filters (Whatman®) and stored at −20 °C until analysis. Inside the bloom, only 5–50 mL water samples were filtered. Chlorophyll was extracted in 10 mL of 90% acetone in the dark at 4 °C for 12 h and analysed by monochromatic spectrophotometry (Aminot and Kérouel, 2004). Microphytoplankton (>20 µm) abundance and community diversity were assessed using an inverted microscope (Zeiss, Axio Observer). One-litre water samples were fixed with Lugol iodine solution (2% f.c.) and stored in the dark at 4 °C. Samples were gently homogenised before settling in 10 mL sub-sample for >12 h in Hydro-Bios counting chambers (Utermöhl, 1958). Limits of quantification was 100 cells L^{-1}. In addition, non-fixed 10 mL sub-samples were observed under light microscopy with the aim of confirming the identification of *L. chlorophorum*. Samples collected inside the bloom were diluted 10 times with filtered seawater (0.2 µm). The relative abundance of the main microphytoplankton genera or species (≥3%) that were clearly identifiable by light microscopy (dinoflagellates, diatoms, cryptophyceae) were represented. Other genera of these groups as well as ciliophora, euglenoidea and prymnesiophyceae were pooled into a group named "Other".

2.5. Satellite data and processing

Previous studies have demonstrated that blooms of *L. chlorophorum* can be detected from satellite remote sensing (Sourisseau et al., 2016; Rodríguez-Benito et al., 2020). Satellite remote sensing can detect phytoplankton in the top layer of the water column, from the surface down to the penetration depth (which roughly corresponds to the Secchi depth). Using *in situ* reflectance measurements, the penetration depth was estimated to vary from 2.6 m in bloom areas where *L. chlorophorum* was highly concentrated, to 19 m outside the bloom waters (Lee et al., 2005).

In the present study, two types of satellite data were used to study the spatial distribution of *L. chlorophorum* during the bloom event in 2019 (see sampling map in the Results section). First, a Landsat-8 (L8) image from July 9, 2019 was selected because it was acquired on the same day as the bloom samples. Although L8 did not offer the optimal spectral resolution to accurately detect phytoplankton blooms, it was still useful to roughly observe patches of high [Chl*a*] at a spatial resolution of 30 m

(Caballero et al., 2020). L8 data were processed using the POLYMER atmospheric correction (Steinmetz et al., 2011), and [Chl*a*] was roughly estimated using the OC3 algorithm (O'Reilly et al., 1998).

Second, satellite images from the Sentinel-2 (S2) mission were used to monitor the bloom's spatial distribution and estimate its surface extent in summer 2019. Due to its high spatial resolution (20 m), revisit time (5 days), and radiometric specifications (10 spectral bands in the visible and near-infrared (NIR) spectral domain), S2 is able to detect phytoplankton blooms in optically complex coastal waters (Caballero et al., 2020). Top-of-atmosphere Level-1C data were downloaded from the Copernicus Open Access Hub and corrected from the atmospheric signal to compute the remote-sensing reflectance (R_{rs}). Three distinct methods of atmospheric correction (AC) were used, and the estimation of the bloom's surface area was eventually computed as the average from the three methods. The combination of several AC methods was chosen here to filter out radiometric uncertainties and provide a robust estimation of the bloom extent from satellite data. In complement to Sen2cor, the default AC implemented by the European Space Agency (Main-Knorn et al., 2017), two other common AC methods were used: POLYMER (Steinmetz et al., 2011) and GRS (Harmel et al., 2018).

A visual inspection of the S2 imagery over the study area from May to August 2019 was performed to select all images showing a green discoloration typical of a *L. chlorophorum* bloom (Siano et al., 2020). Only images showing a conspicuous colour were selected and further processed. Selected images were mostly cloud free and made it possible to accurately detect the bloom's spatial distribution and to compute its areal extent. Partially cloudy images were not used in quantitative analyses but were still useful to investigate bloom temporal dynamics. Bloom detection was performed using an NIR-to-red band ratio algorithm (Gilerson et al., 2010). The reflectance peak near 700 nm is a well-known feature of Chl*a*-rich waters (Gitelson, 1992), and the ability of the $R_{rs}(705)/R_{rs}(665)$ ratio to detect high concentration of chlorophyll-*a* (typically >7 µg L^{-1}) has been previously demonstrated (Lavigne et al., 2021). Red-edge algorithms are known to perform satisfactorily in coastal turbid waters due to the influence of the Chl*a* absorption band around 675 nm as well as the limited interference of non-algal particles (Gernez et al., 2017; Zeng and Binding, 2019) on the NIR-to-red band-ratio. A radiometric threshold of $R_{rs}(705)/R_{rs}(665) >$ 1.05 was used here as a bloom indicator for *L. chlorophorum*. This threshold was obtained empirically by comparing each cloud-free S2 image with the R_{rs} spectra of 50 pixels located inside the bloom *vs.* 50 pixels outside the bloom. While a recent satellite study of a massive *L. chlorophorum* bloom in southern Chile (Rodríguez-Benito et al., 2020) used a threshold corresponding to $R_{rs}(705)/R_{rs}(665) > 1$, we applied a more conservative threshold to reduce the number of false positives. An additional radiometric criterion was further used to detect *L. chlorophorum* using its typical green reflectance peak near 560 nm (Sourisseau et al., 2016). Using the same empirical method, we determined that a threshold of $R_{rs}(560)/R_{rs}(490) > 1.2$ improved the discrimination between bloom and non-bloom areas; the combination of both thresholds allowing to efficiently detect green seawater discoloration pixels, even among the optically complex waters of the Vilaine estuary. Floating macroalgae was excluded using a radiometric threshold in the NIR (e.g., $R_{rs}(865) < 0.01$, Qi and Hu, 2021). Finally, a geometric mask was applied to remove submerged macroalgae surrounding shallow rocky shores, and mudflats where microphytobenthos biofilms could be visible below clear shallow waters.

2.6. Statistical analyses

The spatial distribution of biological and physicochemical parameters during the bloom event was represented by a section scope using the software Ocean Data View (ODV) 5.3.0 (Schlitzer, 2020). As the number of samples per group of variables was low (n < 10), the hypotheses of normal distribution (Shapiro-Wilk test) and homoscedasticity of residuals (Bartlett test) were not verified. The Spearman correlation

matrix was calculated for all parameters at the subsurface and water-sediment interface. Statistical analyses were performed using R software 3.6.1 (R Core Team, 2019).

3. Results

3.1. *Lepidodinium chlorophorum* seasonal variation in 2019

From May to December 2019 (Fig. 2A-U), *L. chlorophorum* was observed both at subsurface and water-sediment interface at the three sampling stations (Fig. 2S, T, U and Fig. S1). The highest abundances were recorded at the Fmax depth (Table 1) or at the water-sediment interface. Indeed, the abundance of *L. chlorophorum* represented 55% of total biomass at the Fmax depth on July 22 at Nord Dumet (2.6×10^5 cells L^{-1} at 10.5 m; Table 1). At the Ouest Loscolo station, the maximal abundance was measured on July 22 (1.9×10^5 cells L^{-1} at the water-sediment interface; Fig. 2T) and on August 6 at the station Men er Roue (5.0×10^5 cells L^{-1} at 5.6 m; Table 1).

At the Nord Dumet station, data from the MOLIT buoy showed a strong decrease in oxygen concentration on July 27 at the water-sediment interface (2.4 mg L^{-1}; Fig. S2A), following high *L.*

Table 1

Abundances of *L. chlorophorum* recorded at the fluorescence maximum depth (Fmax) in 2019 at Nord Dumet, Ouest Loscolo and Men er Roue stations.

Station	Date	*L. chlorophorum* (cells L^{-1})	Depth (m)
Nord Dumet	June 11, 2019	1.3×10^3	6.5
Nord Dumet	July 08, 2019	9.0×10^2	13.0
Nord Dumet	July 22, 2019	2.6×10^5	10.5
Nord Dumet	September 09, 2019	0	11.0
Ouest Loscolo	September 09, 2019	0	6.7
Men er Roue	August 06, 2019	5.0×10^5	5.6

chlorophorum abundance (2.6×10^5 cells L^{-1} at 10.5 m), [Chl*a*] (7.3 µg L^{-1}; Fig. 2P), and [POC] (39 µM; Fig. 2M) registered on July 22 at the Nord Dumet station. In addition, an increase in [TEP] was measured at the water-sediment interface between August 6 (1028 µg Xeq L^{-1}) and August 20 (2882 µg Xeq L^{-1}; Fig. 2J). One month earlier than this bloom (June 7), an increase in the Vilaine River flow was observed (Fig. S3). During this period, the average flow was higher (39 m^3 s^{-1}) than the usual summer average (10 m^3 s^{-1}), with a maximum of 69 m^3 s^{-1} (Fig. S3). The freshwater input subsequently reached station Nord Dumet, as suggested by the subsurface salinity decrease on June 17
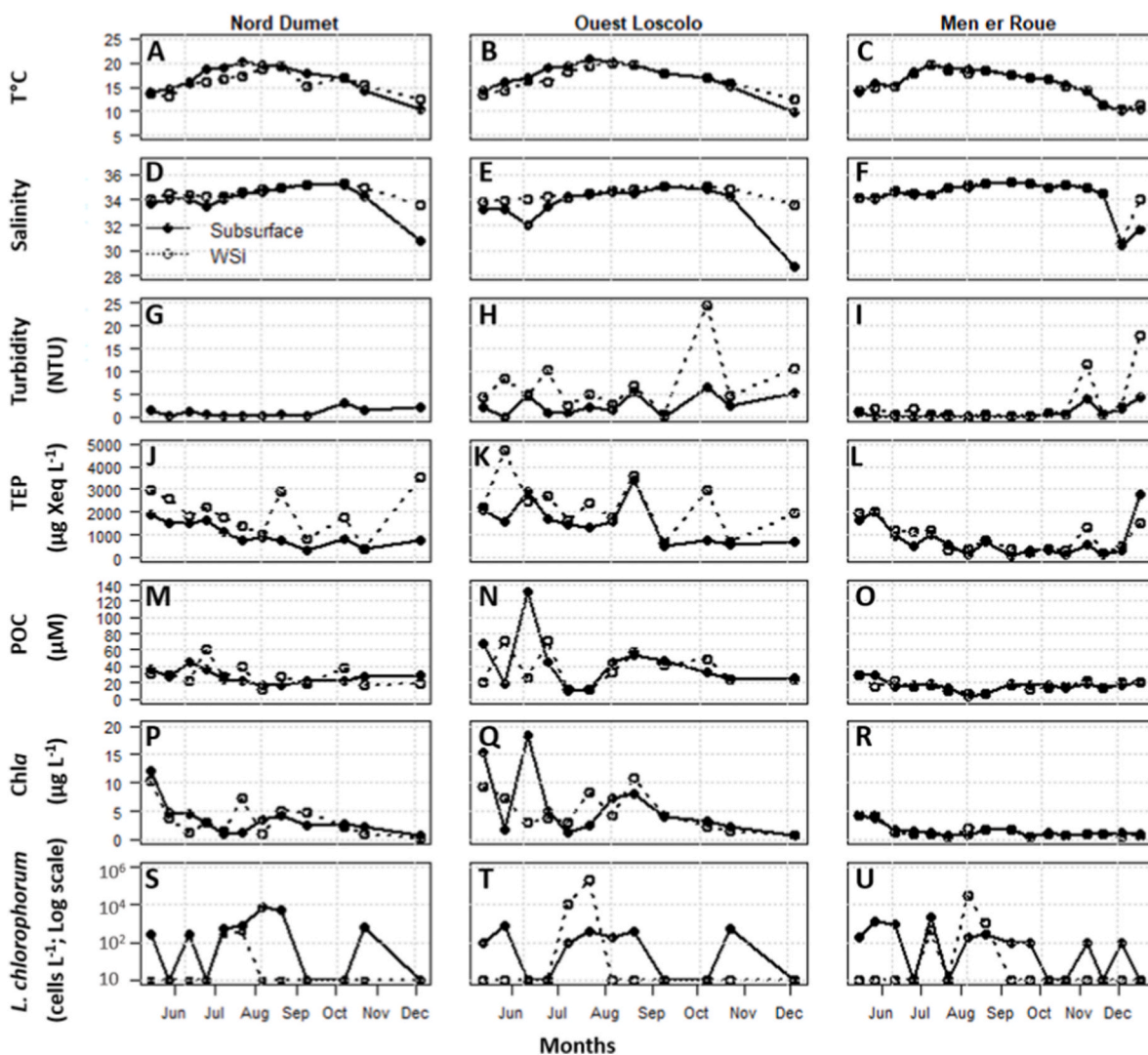

Fig. 2. Variations in hydrological parameters associated with phytoplankton recorded in 2019 at the three sampling stations of the Vilaine Bay (Ouest Loscolo, Nord Dumet) and Quiberon Bay (Men er Roue). Abundances of *L. chlorophorum* (cells L^{-1}) are represented in logarithmic scale. Solid lines represent values measured at the subsurface, and dashed lines represent values obtained at the water-sediment interface (WSI). Values measured at the Fmax depth are not included in the figure and are presented in Table 1.

(Fig. 2D and Fig. S2B). Then, water column thermal stratification occurred from June 26 to July 22, with higher temperatures at the subsurface than at the water-sediment interface (Fig. 2A and Fig. S2C).

The freshwater input was also observed at station Ouest Loscolo, as shown by the salinity decrease in June–July (32.0; Fig. 2E) and the subsurface increase in nutrient concentrations ([NO$_3$+NO$_2$] = 5.7 μM; [DIP] = 0.27 μM; [DSi] = 8.8 μM; Fig. S4). This event was followed on July 22 by an increase in the abundance of *L. chlorophorum* (1.9×10^5 cells L^{-1}; Fig. 2T and Fig. S1D) and [Chl*a*] (8.2 μg L^{-1}; Fig. 2Q) at the water-sediment interface.

In the bay of Quiberon, the station Men er Roue was less influenced by freshwater inputs than the stations of Vilaine Bay and the salinity remained stable around 34 throughout the summer (Fig. 2F). However, a *L. chlorophorum* bloom was observed at the Fmax depth (5.0×10^5 cells L^{-1}; Table 1) and at the water-sediment interface (3.1×10^4 cells L^{-1}; Fig. 2U and Fig. S1F) on August 6, when a thermocline was recorded.

3.2. Analysis of a water discoloration

3.2.1. Spatial dynamics of a water discoloration

Green seawater discolorations were conspicuously visible on Sentinel-2 images (Fig. 3) during the studied bloom event. *In situ* measurements performed within the green seawater discoloration (see below) confirmed that the bloom visible on the S2 images was

dominated by *L. chlorophorum*, at surface concentration $> 10^6$ cells L^{-1} in the greenest waters. The high spatial resolution (20 m) of S2 images made possible to study surface distribution over the whole study area, thus usefully complementing station-based monitoring (see 3.1). While satellite monitoring was occasionally hampered by cloud cover, the screening of cloud-free S2 observations suggested that the bloom started around mid-June and had vanished by late July/early August (Table 2). The influence of tidal circulation appeared to be a primary driver of the bloom spatial structure: patches of high chlorophyll concentration were transported inside the Vilaine Estuary at high tide (Fig. 3A and B) and moved seaward during ebb (Fig. 3C and D). At low tide, the bloom was concentrated along a narrow frontal zone outside the estuary (Fig. 3E and F). During the bloom event, the bloom surface area varied from 2.37 to 12.95 km^2 with a maximum around late June–early July (Table 2).

In situ sampling made it possible to document the composition of the microphytoplankton community within the green seawater discoloration patch on July 9, 2019. Three stations (St1-3) of the radial sampling were located in extremely green waters, as highlighted by both satellite and *in situ* observations (Fig. 3G and H), whereas the remaining sampling stations (St4-6) were located outside the bloom (Fig. 3G). Analyses of the microphytoplankton community composition confirmed that the bloom to a high relative abundance of *L. chlorophorum* (Fig. 4). Within the bloom, *L. chlorophorum* represented more than 95% of total microphytoplankton abundance at both sampling depths (Fig. 4). Outside the
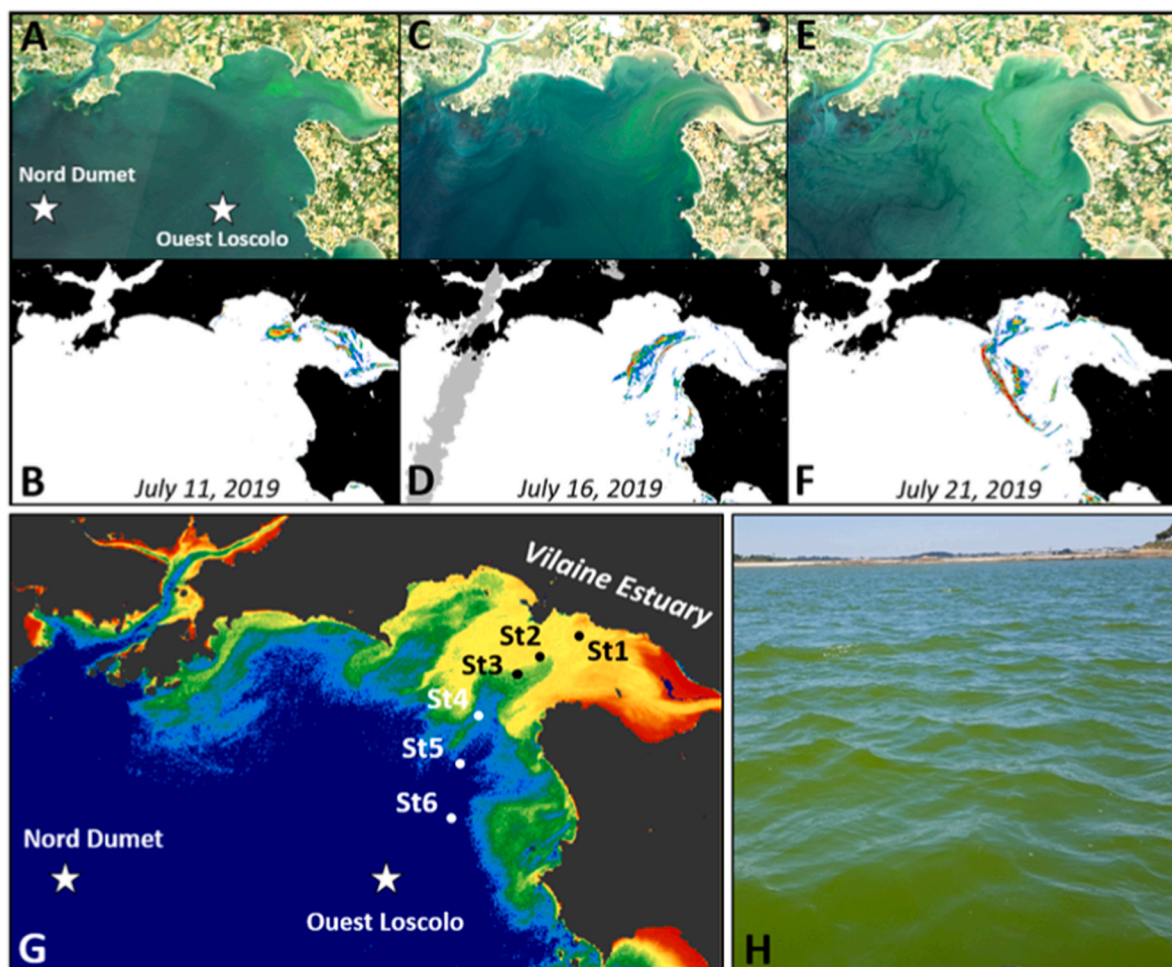

Fig. 3. (**A–F**) Examples of Sentinel-2 images (11, 16, and July 21, 2019) acquired during the green seawater discoloration in summer 2019. Upper panel: RGB images; lower panel: the reflectance ratio $R_{rs}(705)/R_{rs}(665)$ is shown as a proxy of chlorophyll *a* concentration. (**G**) Location of regular stations in the Vilaine Bay, as well as the additional stations specifically sampled during the bloom field experiment on July 9, 2019. The map shows a qualitative estimate of the chlorophyll *a* concentration estimated from the Landsat-8 image acquired July 9, 2019. (**H**) Field picture of green seawater discoloration caused by *Lepidodinium chlorophorum*. (For interpretation of the references to color in this figure legend, the reader is referred to the Web version of this article.)

Table 2

Satellite-derived estimation of bloom surface using Sentinel-2 images (NA = Bloom visible; surface not computed due to cloud cover), the tidal phase, and the water height difference compared to low tide were obtained from the data of the Oceanographic and Hydrological Service of the French National Navy (SHOM).

Date	Bloom surface (km^2)	Tide type	Water height difference compared to low tide (m)	Tidal phase
June 16, 2019	NA	spring	1.72	flow tide
June 21, 2019	2.67 (±1.08)	neap	0.44	ebb tide
June 26, 2019	12.95 (±1.66)	neap	1.89	high tide
July 01, 2019	NA	spring	1.72	flow tide
July 06, 2019	11.12 (±4.75)	spring	0.61	ebb tide
July 11, 2019	2.46 (±1.14)	neap	3.00	high tide
July 16, 2019	2.37 (±0.98)	neap	1.01	flow tide
July 21, 2019	2.91 (±1.03)	neap	0.57	ebb tide

NB: In the shallow waters (depth <4 m) where the bloom occurred, vertically-resolved field sampling documented high abundance of *L. chlorophorum* from the surface down to about 2 m (Fig. 5A), which is roughly similar to the penetration depth of satellite measurement (about 2.6 m). Furthermore, during that period, samples from the offshore stations (i.e., Nord Dumet and Men er Roue, Fig. S1) did not show significant amounts of *L. chlorophorum* at depths. It is therefore likely that Sentinel-2 detected most of the bloom biomass.

bloom, *L. chlorophorum* was relatively less abundant at the subsurface (relative abundance <23%, Fig. 4A) than at the water-sediment interface. At St4, while *L. chlorophorum* dominated the microphytoplankton community at the water-sediment interface (>94%; Fig. 4B), other dinoflagellates, such as *Gymnodinium* spp., *Gyrodinium* spp., *Scrippsiella* spp., and *Protoperidinium* spp., dominated at the subsurface (Fig. 4A). From St4 seaward, the proportion of dinoflagellates within the microphytoplankton community tended to decrease, with *Leptocylindrus* spp. The most dominant diatom genus at the subsurface at St6 (Fig. 4A). The diatom genus *Chaetoceros* spp. and the dinoflagellate *Dinophysis* spp. were only detected (≥3%) at the water-sediment interface at St6 (Fig. 4B).

Following these changes in the phytoplankton community, both Chl*a* and *L. chlorophorum* concentrations sharply declined from nearshore to offshore. The highest phytoplankton biomass was recorded at St1, with [Chl*a*] ranging from 38 µg L^{-1} at the water-sediment interface to 73 µg L^{-1} at the subsurface (Fig. S5A). *Lepidodinium chlorophorum* abundance

was up to 2000-fold higher at the subsurface inside (St1) than outside the bloom (St6; Fig. 5A). The highest abundance was recorded at the subsurface at St1 (8.9×10^6 cells L^{-1}), and the lowest was observed at the subsurface at St6 (4.1×10^3 cells L^{-1}; Fig. 5A). At the water-sediment interface, *L. chlorophorum* was observed throughout the sampled area, with values ranging from 3.2×10^6 cells L^{-1} within the bloom (St1) to 53.4×10^3 cells L^{-1} outside the bloom (St6, Fig. 5A).

A decreasing temperature gradient was observed seaward from St1 ($19.6 \pm 0.9\,°C$) to St6 ($18.4 \pm 0.8\,°C$) at both sampling depths (Fig. 5B). In contrast, salinity increased seaward, both in subsurface waters (from 32.4 to 34.1) and at the water-sediment interface (from 33.8 to 34.0; Fig. 5C). While [DSi] declined gradually along the salinity gradient from 21 µM at St1 to 13.7 µM at St6 at the subsurface (Fig. 5D), other inorganic nutrient concentrations followed a spatial pattern similar to that observed for *L. chlorophorum* abundance. Moreover, the highest [NO_2] (Fig. S5B), [NH_4] (Fig. 5E), and [DIP] (Fig. 5F) were recorded at the subsurface within the bloom (at St1, [NO_2], [NH_4], and [DIP] were 0.14, 0.48, and 1.63 µM, respectively). In contrast, [NO_3] was very low throughout the sampling area, with values remaining below the limit of quantification (i.e., LQ < 0.5 µM) at the six sampling stations and both depths (Fig. S5C).

3.2.2. Biogeochemical characteristics of the water discoloration

[DON] (Fig. 5G) and [DOC] (Fig. S5D) showed a spatial pattern similar to that of *L. chlorophorum* abundance, with a subsurface maximum at St1 (66 and 655 µM, respectively). Subsequently, [DON] and [DOC] decreased sharply seaward, with the lowest values at St6 ([DON] < 12 µM; [DOC] < 200 µM). The DOC/DON ratio was lower inside (St1, subsurface: 9.9; water-sediment interface: 7.4) than outside the bloom (St6, subsurface: 16.0; water-sediment interface: 13.8; Table S1). In contrast, the POC/PON ratio was higher inside (St1, subsurface: 11.5; water-sediment interface: 11.2) than outside the bloom (St6, subsurface: 7.1; water-sediment interface: 6.7; Table S1). [POC] and [PON] (Figs. S5E and F) followed the same pattern as the dissolved fraction. The highest [POC] and [PON] were measured at the subsurface at St1 (1163 and 101 µM, respectively). The highest [TEP] was recorded at St1, ranging from 3579 at the water-sediment interface to 24446 µg Xeq L^{-1} at the subsurface (Fig. 5H). The [TEP] also dramatically decreased seaward and reached a very low value at St6, with concentrations of 677 and 455 µg Xeq L^{-1} at the water-sediment interface and subsurface, respectively (Fig. 5H). At the subsurface, [TEP] was up to 50-fold higher inside (St1) than outside the bloom (St6).

To establish the carbon signature of an *L. chlorophorum* bloom, a conversion factor of 0.51 was used to convert from µg Xeq to µgC (TEP-C; Passow and Engel, 2001). Considering the TEP-C and POC values
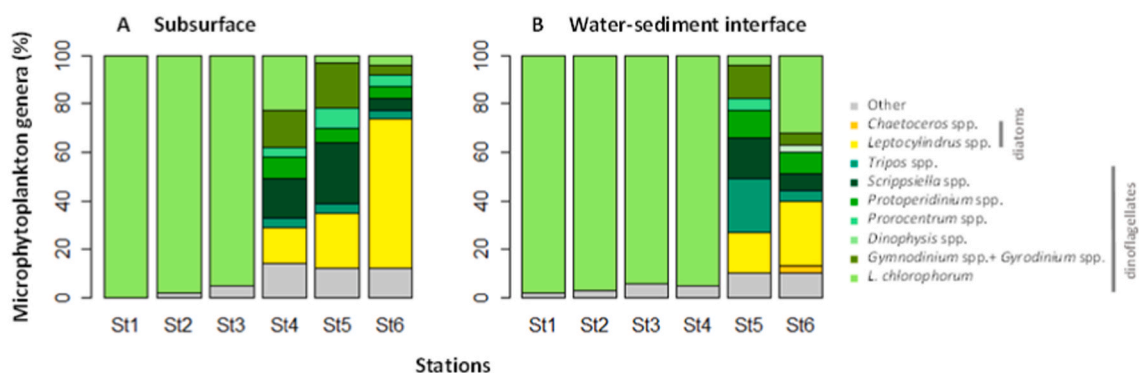

Fig. 4. Relative abundances (%) of the main microphytoplankton genera or species observed inside (St1, St2, St3) and outside (St4, St5, St6) the green seawater discoloration (**A**) at the subsurface and (**B**) water-sediment interface. (For interpretation of the references to color in this figure legend, the reader is referred to the Web version of this article.)
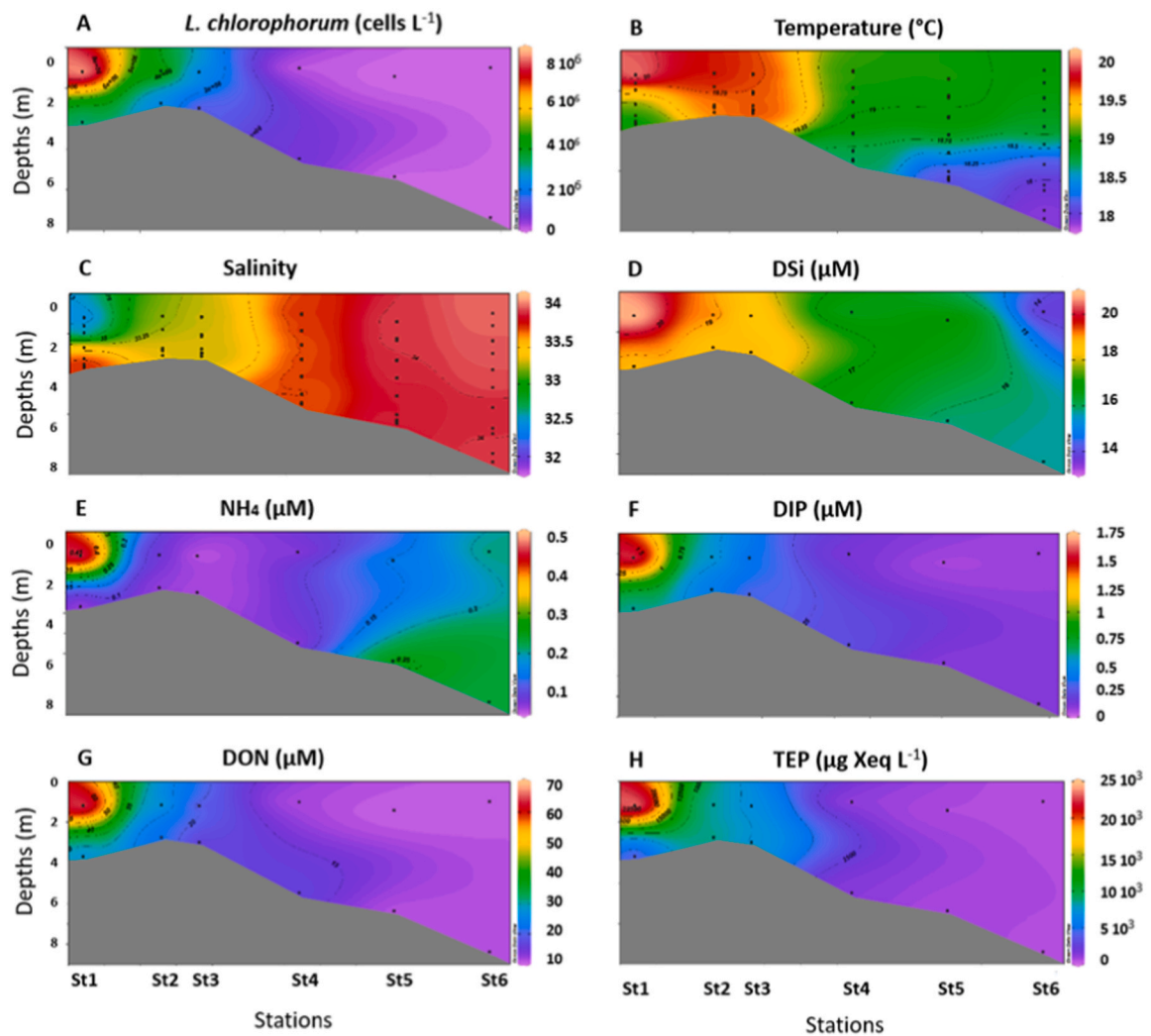
Fig. 5. Spatial distribution of biological and physicochemical parameters: (**A**) *L. chlorophorum* concentrations, (**B**) temperature, (**C**) salinity, (**D**) silicates (DSi), (**E**) ammonium (NH$_4$), (**F**) phosphates (DIP), (**G**) dissolved organic nitrogen (DON), and (**H**) transparent exopolymer particles (TEP), measured inside (St1, St2, St3) and outside (St4, St5, St6) the bloom (Ocean Data View, 5.3.0).

reported in this study, the TEP-C contribution to the POC pool (TEP-C% POC) was estimated. In subsurface waters, the TEP-C ranged from 3509 to 12468 µg L^{-1} inside the bloom and from 232 to 467 µg L^{-1} outside the bloom. The TEP-C%POC contribution was higher inside (59–89%:St1, St2, St3) than outside (44–61%:St4, St5, St6) the bloom.

The SEP from the St1 supernatant, collected at the subsurface inside the bloom, were mainly composed of proteins and neutral monosaccharides. Both galactose and glucose were predominant over other neutral monosaccharides that were also detected, such as rhamnose and mannose. For electrophoresis gels (Fig. S6), the St1 supernatant presented a similar profile (a polydisperse blot) to galactan sulphate (molecular weight; MW 80000) and dextran sulphate (MW 50000). The absence of a smear in the stacking gel, as observed with dextran sulphate (MW 500000), indicated that no high molecular weight chains were present in the sample. The SEP molecular weight of St1 was below 100,000. The colour intensity of the St1 supernatant was close to that of galactan sulphate, suggesting a similar sulphur content close to 8%. Moreover, its electrophoretic mobility and profile indicated a similar molecular weight and polydispersity to those of standard galactan sulphate. The ATR-FTIR spectra were characteristic of polysaccharides with a broad absorption band attributed to the O–H stretching vibration above 3000 cm^{-1} and an intense absorption between 1650 and 1050

cm^{-1}, corresponding to characteristic bands of polysaccharides (Fig. S7). Moreover, at 2931 cm^{-1}, a band assigned to the C–H symmetrical stretching vibration was also present. The presence of sulphate groups was confirmed in all polysaccharides with strong absorption bands at 1230 cm^{-1}, which corresponded to the asymmetrical stretching vibration of the sulphate ester groups (S=O), and at 813 and 815 cm^{-1}, which was assigned to the C–O–S vibration; these bands were more intense in the highly sulphated dextran sulphate.

3.2.3. Relationship of L. chlorophorum with other biogeochemical parameters

Lepidodinium chlorophorum abundance was positively correlated with [Chl*a*], [DIP], [NO$_2$] and [DON] (r > 0.90; p < 0.05) at the subsurface (Table S2A). [TEP] was also correlated with cell abundance (r = 0.94; p < 0.05) and [POC] (r = 1; p < 0.05) at the subsurface (Table S2A). In contrast, [NH$_4$] was negatively correlated with [Chl*a*] and dinoflagellate abundance (r = −0.89; p < 0.05) at the water-sediment interface (Table S2B). Overall, *L. chlorophorum* concentrations were positively correlated with temperature, concentration of dissolved and particulate organic matter, and [NH$_4$] and [DIP].

4. Discussion

The dinoflagellate *L. chlorophorum* is an example of a phytoplankton species causing green seawater discolorations worldwide (Honsell and Talarico, 2004; Iriarte et al., 2005; McCarthy, 2013; Gárate-Lizárraga et al., 2014; Rodríguez-Benito et al., 2020). The present study described the seasonal variation of this species in the southern Brittany coast and characterized some biogeochemical properties of a bloom event of this species, for the first time.

4.1. Physical factors influencing L. chlorophorum bloom dynamics

Our results confirmed that *L. chlorophorum* occurs from May to November in South Brittany (Sournia et al., 1992; Sourisseau et al., 2016; Siano et al., 2020). While the environmental parameter variations observed in 2019 are congruent with the main seasonal dynamics generally recorded in the Vilaine and Quiberon bays (Fig. S8), the year 2019 was characterised by a significant increase in the Vilaine River flow during late May - early June (Fig. S3). This intermittent freshwater input and the increase in surface water temperature contributed to the establishment of water column stratification, creating favourable conditions for the development of the bloom. Indeed, the highest *L. chlorophorum* concentration and bloom surface extent (Table 2) were recorded in July when the water column was stratified.

Water-mass stratification is considered an essential physical condition that dinoflagellates require to bloom (Margalef, 1978; Smayda, 2002a). Previous studies highlighted the occurrence of high densities of *Alexandrium catenella* (Giacobbe et al., 1996; Anderson et al., 2012; Yamamoto et al., 2013; Condie et al., 2019) and *Dinophysis* sp. (Velo-Suárez et al., 2009; Diaz et al., 2021) in subsurface thin layers, in correspondence with the pycnocline (Nielsen et al., 1990; Kononen et al., 2003; Lips et al., 2010). In these layers, primary production can exceed surface production (Richardson et al., 2000). For *L. chlorophorum*, Sourisseau et al. (2016) observed high densities at the pycnocline in stratified areas. Our study showed that the influence of the Vilaine River and the establishment of thermal stratification affect the development of this species in the water column, corroborating previous studies suggesting that *L. chlorophorum* blooms could be correlated with freshwater input from rivers (Sournia et al., 1992; Karasiewicz et al., 2020). These environmental conditions correspond to the Type I habitat (shallow, nutrient-enriched, nearshore waters) described by Smayda (2002b), in which small gymnodinoid species, such as *L. chlorophorum*, tend to predominate.

The highest abundances of *L. chlorophorum* were recorded at the Fmax depth or at the water-sediment interface, suggesting that this species could migrate vertically through the water column (Sourisseau et al., 2016). As demonstrated for other dinoflagellates (Dagenais-Bellefeuille and Morse, 2013; Glibert et al., 2016), *L. chlorophorum* could use nutrients located below the pycnocline. Moreover, mixotrophic organisms are able to predate nano-flagellates and bacteria located below the pycnocline. However, to our knowledge, vertical migration as well as mixotrophy have not been clearly established for *L. chlorophorum*, but just supposed (Hansen and Moestrup, 2005; Ng et al., 2017; Liu et al., 2021).

As wind speed (<8 knots; mainly from N to NE sectors), vertical mixing (neap tide period) and Vilaine River flow remained low for more than one month, the bloom event documented in the present study could then be considered an ideal case to study the effects of tidal variations on phytoplankton distribution in a macro tidal estuary. Satellite observations highlighted the influence of short-scale variability on the bloom surface extent and spatial distribution associated with semi-diurnal tidal dynamics. The location of *L. chlorophorum* patches detected by high-resolution remote sensing was consistent with biophysical modelling, where the accumulation of phytoplankton biomass is driven by the interplay between local processes, such as horizontal transport along the main river channel, cross-estuary oscillations, lateral sloshing (Lucas et al., 1999a), and variability in phytoplankton growth rates and population dynamics (Lucas et al., 1999b). Red-edge algorithms are not affected by changes in turbidity associated with river plumes, and the high-resolution Sentinel-2 observations proved useful in estimating the temporal and spatial dynamics of the green seawater discoloration in the first optical layer (i.e. the top 3 m) during summer. However, the detection of relatively high *L. chlorophorum* abundance at the depth of fluorescence maximum and/or below the pycnocline suggest that a significant part of the bloom's biomass may remain undetectable from passive satellite remote sensing.

4.2. Biogeochemical specificity of L. chlorophorum blooms

The distribution of TEP in marine ecosystems results from the balance between sources, consumption by organisms, and sinks (Alldredge et al., 1998; Passow, 2002). In 2019, the seasonal [TEP] measured in the Vilaine and Quiberon bays were in the highest range of values recorded in coastal seawaters at different locations of the world (Passow, 2002). Higher [TEP] are frequently reported in productive areas or during blooms (Engel, 2004; Corzo et al., 2005; Prieto et al., 2006; Ortega-Retuerta et al., 2009, 2010; Bar-Zeev et al., 2011). For *L. chlorophorum*, enrichment experiments on the natural population have shown that [TEP] increased by a factor of 3 in DIP enrichment and by a factor of 1.9 in both DIN and DIN/DSi enrichments (Serre-Fredj et al., 2021). Our study confirmed that a *L. chlorophorum* bloom produce a high [TEP] *in situ*. Moreover, subsurface concentrations of *L. chlorophorum* and [TEP] measured inside the bloom were similar to the values obtained by Roux et al. (2021) under laboratory conditions (12 × 10^6 cells L^{-1} and 17 × 10^3 μg Xeq L^{-1}, respectively). In addition, SEP collected inside the bloom were mainly composed of proteins, glucose and galactose, and the presence of sulphated exopolysaccharides was observed. These results corroborate the SEP composition previously found under laboratory conditions (Roux et al., 2021). Therefore, *L. chlorophorum* produce a sulphated exopolysaccharide composed mainly of galactose, confirming that galactose-based exopolysaccharide is a common characteristic among dinoflagellates (Hasui et al., 1995; Yim et al., 2007; Mandal et al., 2011). While sources of TEP and SEP from terrestrial freshwater inputs cannot be completely excluded (Attermeyer et al., 2019), these results reported high TEP concentrations within a bloom and suggest that *L. chlorophorum* is the main responsible for this production.

Subsurface [DIP] and [NH$_4$] were drastically higher inside than outside the bloom. Concentrations recorded on July 8, 2019 at the most upstream station in the Vilaine Estuary (salinity = 32.0) were used to evaluate the origin of these inorganic nutrients (Fig. S9). The behaviour of DSi along the salinity gradient was conservative (Fig. S9A) while those of DIP and NH$_4$ denote a production inside the bloom (Figs. S9B and C). These results suggest that important nutrient recycling occur inside the bloom. This hypothesis is supported by the high subsurface dissolved organic matter concentrations. Indeed, DON may be released by exudation from phytoplankton and bacteria (Bronk and Ward, 1999; Diaz and Raimbault, 2000) or from cell death or viral lysis (Fuhrman, 1999). While allochthonous sources of DON from terrestrial runoff, leaching from plant detritus and soils into streams, rivers, and sediments, and atmospheric deposition cannot completely be excluded, other parameters tend to support the hypothesis of intense remineralisation processes inside the bloom.

The POC/PON ratio was higher than the Redfield ratio (C/N = 106/16; Redfield, 1958) inside the bloom, suggesting an accumulation of TEP and detrital organic matter produced by *L. chlorophorum* in subsurface waters. In contrast, the DOC/DON ratio was lower inside than outside the bloom. These results suggest that organic matter, produced by *L. chlorophorum* and maintained in subsurface waters, could provide a microenvironment promoting bacterial development and remineralisation processes (Alldredge and Gotschalkt, 1989; Schapira et al., 2012a, 2012b). Through the microbial loop, bacteria provide regenerated inorganic nutrients (Caron, 1994). Moreover, previous studies suggested

that *L. chlorophorum* could present high ammonium assimilation rates (Iriarte et al., 2005; Karasiewicz et al., 2020). Presumably, inorganic nutrients regenerated by bacterial remineralisation within the bloom might sustain the development of *L. chlorophorum* cells. This could be especially prevalent during calm periods (neap tide and low wind) when the water residence time is longer in the Vilaine Bay (Chapelle et al., 1994). Furthermore, the studied bloom was observed by satellite image for more than one month, confirming bloom duration deduced by citizen observations in this area (Siano et al., 2020). As shown under laboratory conditions (Roux et al., 2021), a strong relationship was suggested between *L. chlorophorum* and its associated bacterial consortia through remineralisation processes within a bloom. The bacterial compartment within a bloom remains to be investigated. However, the microenvironment established within a bloom can attract different types of organisms. Previous studies reported that bacteria, protozoa, phytoplankton and metazoan colonize TEP (Simon et al., 2002; Lyons et al., 2007; Shapiro et al., 2014). As the genus *Lepidodinium* is suspected mixotrophic (Hansen and Moestrup, 2005; Ng et al., 2017; Liu et al., 2021), *L. chlorophorum* could predate also heterotrophic organisms, such as nano-flagellates.

4.3. Potential harmful effects of L. chlorophorum blooms on the environment

TEP aggregation tends to accelerate the sedimentation of organic matter from the surface to the seabed (Passow et al., 2001; Mari et al., 2017; Bittar et al., 2018). As demonstrated in a previous study performed under laboratory conditions (Roux et al., 2021), our results confirmed that TEP produced during a bloom of *L. chlorophorum* were associated with high [POC] *in situ*. Moreover, TEP contribute to carbon export and can represent a significant fraction of the carbon pool in our study, as well as others (Passow et al., 2001; Mari et al., 2017; Bittar et al., 2018). In the estuarine system, Annane et al. (2015) showed that TEP-C combined with phytoplankton-C were major contributors to the carbon pool (41 and 54%, respectively) and significantly contributed to the decrease in oxygen concentration in the bottom layer by respiration/remineralisation processes.

Our observations suggested that the large amount of TEP (carbon-rich) excreted by *L. chlorophorum* could enhance remineralisation processes in the water column and accentuate hypoxia close to the water-sediment interface. Oxygen concentrations measured during summer 2019 supported this hypothesis. Indeed, low oxygen concentrations (2.4 mg L^{-1}) were recorded at the water-sediment interface by the autonomous buoy located at the Nord Dumet station following an *L. chlorophorum* bloom. These low oxygen concentrations could have extensive consequences for marine fauna. For many benthic invertebrates, the hypoxia threshold is about 2.9 mg L^{-1} or less (Herreid, 1980; Rosenberg et al., 1991; Diaz and Rosenberg, 2008). The reduction in feeding activity and oxygen consumption is a commonly observed response to hypoxia in bivalves (Sobral and Widdows, 1997; Hicks and McMahon, 2002). However, more data regarding oxygen concentrations at the water-sediment interface are needed to confirm these results. *In situ* and *in vitro* experiments focused on the interaction between *L. chlorophorum* and bivalves could complete the analyses on the ecological and potentially harmful impact of this dinoflagellate.

5. Conclusions

Coastal blooms of the marine green dinoflagellate *L. chlorophorum* can cause summer green seawater discolorations worldwide. Using an original combination of field sampling and high-resolution satellite remote sensing, the present study characterized phytoplankton spatio-temporal distribution and biogeochemical properties during a massive bloom of this dinoflagellate in the bay of Vilaine, a eutrophic estuary of the French Atlantic coast. *Lepidodinium chlorophorum* occurred from May to November, with very high surface abundance during summer

(June–July). Occasionally, high abundances of *L. chlorophorum* were also recorded at the Fmax depth or deeper. Freshwater inputs (a few weeks before the bloom), sea-surface warming, and thermohaline stratification promoted bloom development. The bloom spatial distribution was then influenced by tidal variability, with seaward and landward movements associated with ebb and flow tide, respectively.

Lepidodinium chlorophorum produced a large amount of TEP (carbon-rich). In addition, the SEP produced by this species were mainly composed of sulphated galactan. The high secretion of extracellular polymeric substances, a biological trait particularly developed by this dinoflagellate in comparison to other species, could confer a specific ecological advantage to *L. chlorophorum*. The production of TEP would enhance bacteria remineralisation, which would provide nutrients to sustain the bloom for a long period, especially during calm conditions (low wind, and persistent water column stratification). TEP could also facilitate mixotrophy by attracting a large number of heterotrophic organisms. However, the large amount of TEP excreted within the bloom could have a harmful effect on the environment, causing marine fauna and cultivated bivalve mortalities through the enhancement of oxygen reduction, especially close to the water-sediment interface. Further studies are needed to investigate the role of bacteria within the bloom and to fully assess the role of green seawater discoloration on oxygen concentration and potential impact on bivalves. These first insights into the ecological properties of *L. chlorophorum* in southern Brittany constitute the baseline for further studies in other ecosystems impacted by this species.

CRediT authorship contribution statement

Pauline Roux: Writing – original draft, Formal analysis, Data curation. **Raffaele Siano:** Writing – review & editing, Conceptualization. **Philippe Souchu:** Writing – review & editing. **Karine Collin:** Visualization, Investigation. **Anne Schmitt:** Visualization, Investigation. **Soazig Manach:** Visualization, Investigation. **Michael Retho:** Visualization, Investigation. **Olivier Pierre-Duplessix:** Visualization, Investigation. **Laetitia Marchand:** Visualization, Investigation. **Sylvia Colliec-Jouault:** Writing – review & editing. **Victor Pochic:** Visualization, Investigation. **Maria Laura Zoffoli:** Writing – review & editing, Investigation. **Pierre Gernez:** Writing – review & editing, Investigation. **Mathilde Schapira:** Supervision, Project administration, Methodology, Funding acquisition, Conceptualization.

Declaration of competing interest

The authors declare that they have no known competing financial interests or personal relationships that could have appeared to influence the work reported in this paper.

Data availability

Data will be made available on request.

satellite data. Pauline Roux, Mathilde Schapira, Raffaele Siano, Karine Collin, Anne Schmitt, Olivier Pierre-Duplessix, Michael Retho, and Soazig Manach are part of GDR PHYCOTOX, a CNRS/IFREMER network on Harmful Algal Blooms (https://www.phycotox.fr/). Finally, the authors thank the anonymous reviewers for their careful reading of our manuscript and their insightful comments and suggestions.

Appendix A. Supplementary data

Supplementary data to this article can be found online at https://doi.org/10.1016/j.ecss.2022.107950.

References

Alldredge, A.L., Gotschalk, C.C., 1989. Direct observations of the mass flocculation of diatom blooms: characteristics, settling velocities and formation of diatom aggregates. Deep-Sea Res. 36 (2), 159–171. https://doi.org/10.1016/0198-0149(89)90131-3.

Alldredge, A.L., Passow, U., Haddock, S.H.D., 1998. The characteristics and transparent exopolymer particle (TEP) content of marine snow formed from thecate dinoflagellates. J. Plankton Res. 20 (3), 393–406. https://doi.org/10.1093/plankt/20.3.393.

Alunno-Bruscia, M., Bourlès, Y., Maurer, D., Robert, S., Mazurié, J., Gangnery, A., Goulletquer, P., Pouvreau, S., 2011. A single bio-energetics growth and reproduction model for the oyster *Crassostrea gigas* in six Atlantic ecosystems. J. Sea Res. 66, 340–348. https://doi.org/10.1016/j.seares.2011.07.008.

Aminot, A., Kérouel, R., 2004. In: Ifremer, Plouzané (Ed.), Hydrologie des écosystèmes marins : paramètres et analyses in French, (France).

Aminot, A., Kérouel, R., 2007. In: Ifremer, Plouzané (Ed.), Dosage automatique des nutriments dans les eaux marines : méthodes en flux continu in French, (France).

Anderson, D.M., Alpermann, T.J., Cembella, A.D., Collos, Y., Masseret, E., Montresor, M., 2012. The globally distributed genus *Alexandrium*: multifaceted roles in marine ecosystems and impacts on human health. Harmful Algae 14, 10–35. https://doi.org/10.1016/j.hal.2011.10.012.

Annane, S., St-Amand, L., Starr, M., Pelletier, E., Ferreyra, G.A., 2015. Contribution of transparent exopolymeric particles (TEP) to estuarine particulate organic carbon pool. Mar. Ecol. Prog. Ser. 529, 17–34. https://doi.org/10.3354/meps11294.

Attermeyer, K., Andersson, S., Catalán, N., Einarsdottir, K., Groeneveld, M., Székely, A.J., Tranvik, L.J., 2019. Potential terrestrial influence on transparent exopolymer particle concentrations in boreal freshwaters. Limnol. Oceanogr. 64, 2455–2466. https://doi.org/10.1002/lno.11197.

Bar-Zeev, E., Berman, T., Rahav, E., Dishon, G., Herut, B., Kress, N., Berman-Frank, I., 2011. Transparent exopolymer particle (TEP) dynamics in the eastern Mediterranean Sea. Mar. Ecol. Prog. Ser. 431, 107–118. https://doi.org/10.3354/meps09110.

Belin, C., Soudant, D., Amzil, Z., 2021. Three decades of data on phytoplankton and phycotoxins on the French coast: lessons from REPHY and REPHYTOX. Harmful Algae, 101733. https://doi.org/10.1016/j.hal.2019.101733.

Bittar, T.B., Passow, U., Hamaraty, L., Bidle, K.D., Harvey, E.L., 2018. An updated method for the calibration of transparent exopolymer particle measurements. Limnol Oceanogr. Methods 16, 621–628. https://doi.org/10.1002/lom3.10268.

Bronk, D.A., Ward, B.B., 1999. Gross and net nitrogen uptake and DON release in the euphotic zone of Monterey Bay, California. Limnol. Oceanogr. 44 (3), 573–585. https://doi.org/10.4319/lo.1999.44.3.0573.

Brown, C.A., Ozretich, R.J., 2009. Coupling between the coastal ocean and yaquina bay, Oregon: importance of oceanic inputs relative to other nitrogen sources. Estuar. Coast 32, 219–237. https://doi.org/10.1007/s12237-008-9128-6.

Cabal, J., González-Nuevo, G., Nogueira, E., 2008. Mesozooplankton species distribution in the NW and N Iberian shelf during spring 2004: relationship with frontal structures. J. Mar. Syst. 72, 282–297. https://doi.org/10.1016/j.jmarsys.2007.05.013.

Caballero, I., Fernández, R., Escalante, O.M., Mamán, L., Navarro, G., 2020. New capabilities of Sentinel-2A/B satellites combined with in situ data for monitoring small harmful algal blooms in complex coastal waters. Sci. Rep. 10, 8743. https://doi.org/10.1038/s41598-020-65600-1.

Caron, D.A., 1994. Inorganic nutrients, bacteria, and the microbial loop. Microb. Ecol. 28 (2), 295–298. https://doi.org/10.1007/BF00166820.

Carstensen, J., Frohn, L.M., Hasager, C.B., Gustafsson, B.G., 2005. Summer algal blooms in a coastal ecosystem: the role of atmospheric deposition versus entrainment fluxes. Estuar. Coast Shelf Sci. 62, 595–608. https://doi.org/10.1016/j.ecss.2004.09.026.

Carstensen, J., Henriksen, P., Heiskanen, A.S., 2007. Summer algal blooms in shallow estuaries: definition, mechanisms, and link to eutrophication. Limnol. Oceanogr. 52 (1), 370–384. https://doi.org/10.4319/lo.2007.52.1.0370.

Chapelle, A., Lazure, P., Ménesguen, A., 1994. Modelling eutrophication events in a coastal ecosystem. Sensitivity analysis. Estuar. Coast Shelf Sci. 39, 529–548. https://doi.org/10.1016/S0272-7714(06)80008-9.

Claquin, P., Probert, I., Lefebvre, S., Veron, B., 2008. Effects of temperature on photosynthetic parameters and TEP production in eight species of marine microalgae. Aquat. Microb. Ecol. 51, 1–11. https://doi.org/10.3354/ame01187.

Cloern, J.E., 1996. Phytoplankton bloom dynamics in coastal ecosystems: a review with some general lessons from sustained investigation of San Francisco Bay, California. Rev. Geophys. 34 (2), 127–168. https://doi.org/10.1029/96RG00986.

Cloern, J.E., Schraga, T.S., Lopez, C.B., 2005. Heat wave bring an unprecedent red tide to san francisco bay. Ocean Sci. 86 (7), 66. https://doi.org/10.1029/2005EO070003.

Cloern, J.E., Jassby, A.D., Thompson, J.K., Hieb, K.A., 2007. A cold phase of the East Pacific triggers new phytoplankton blooms in San Francisco Bay. Proc. Natl. Acad. Sci. USA 104 (47), 18561–18565. https://doi.org/10.1073/pnas.0706151104.

Condie, S.A., Oliver, E.C.J., Hallegraeff, G.M., 2019. Environmental drivers of unprecedented *Alexandrium catenella* dinoflagellate blooms off eastern Tasmania, 2012–2018. Harmful Algae 87, 101628. https://doi.org/10.1016/j.hal.2019.101628.

Core Team, R., 2019. A Language and Environment for Statistical Computing. R Foundation for Statistical Computing, Vienna. https://www.R-project.org.

Corzo, A., Rodríguez-Gálvez, S., Lubian, L., Sangrá, P., Martínez, A., Morillo, J.A., 2005. Spatial distribution of transparent exopolymer particles in the Bransfield Strait, Antarctica. J. Plankton Res. 27 (7), 635–646. https://doi.org/10.1093/plankt/fbi038.

Dagenais-Bellefeuille, S., Morse, D., 2013. Putting the N in dinoflagellates. Front. Microbiol. 4, 369. https://doi.org/10.3389/fmicb.2013.00369.

Diaz, F., Raimbault, P., 2000. Nitrogen regeneration and dissolved organic nitrogen release during spring in a NW Mediterranean coastal zone (Gulf of Lions): implications for the estimation of new production. Mar. Ecol. Prog. Ser. 197, 51–65. https://www.jstor.org/stable/24855744.

Diaz, R.J., Rosenberg, R., 2008. Spreading dead zones and consequences for marine ecosystems. Science 321, 926–929. https://doi.org/10.1126/science.1156401.

Diaz, P.A., Perez-Santos, I., Alvarez, G., Garreaud, R., Pinilla, E., Diaz, M., Sandoval, A., Araya, M., Alvarez, F., Rengel, J., Montero, P., Pizarro, G., Lopez, L., Iritarte, L., Igor, G., Reguera, B., 2021. Multiscale physical background to an exceptional harmful algal bloom of *Dinophysis acuta* in a fjord system. Sci. Total Environ. 773, 145621 https://doi.org/10.1016/j.scitotenv.2021.145621.

Elbrächter, M., Schnepf, E., 1996. *Gymnodinium chlorophorum*, a new, green, bloom-forming dinoflagellate (Gymnodiniales, Dinophyceae) with a vestigial prasinophyte endosymbiont. Phycologia 35 (5), 381–393. https://doi.org/10.2216/i0031-8884-35-5-381.1.

Engel, A., 2004. Distribution of transparent exopolymer particles (TEP) in the northeast Atlantic Ocean and their potential significance for aggregation processes. Deep-Sea Res., Part A I 51 (1), 83–92. https://doi.org/10.1016/j.dsr.2003.09.001.

Fuhrman, J.A., 1999. Marine viruses and their biogeochemical and ecological effects. Nature 399, 541–548. https://doi.org/10.1038/21119.

Gárate-Lizárraga, I., Muñetón-Gómez, M.S., Pérez-Cruz, B., Díaz-Ortíz, J.A., 2014. Bloom of *Gonyaulax spinifera* (dinophyceae: gonyaulacales) in ensenada de la Paz Lagoon, Gulf of California. CICIMAR Oceánides 29 (1), 11–18. https://doi.org/10.37543/oceanides.v29i1.130.

Garvetto, A., Nézan, E., Badis, Y., Bilien, G., Arce, P., Bresnan, E., Gachon, C.M.M., Siano, R., 2018. Novel widespread marine oomycetes parasitising diatoms, including the toxic genus pseudo-nitzschia: genetic, *morphological,* and ecological characterisation. Front. Microbiol. 9, 1–19. https://doi.org/10.3389/fmicb.2018.02918.

Gavalás-Olea, A., Álvarez, S., Riobó, P., Rodríguez, F., Garrido, J.L., Vaz, B., 2016. 19,19′-Diacyloxy signature: an atypical Level of structural evolution in carotenoid pigments. Org. Lett. 18, 4642–4645. https://doi.org/10.1021/acs.orglett.6b02272.

Gernez, P., Doxaran, D., Barillé, L., 2017. Shellfish aquaculture from space: potential of Sentinel2 to monitor tide-driven changes in turbidity, chlorophyll concentration and oyster physiological response at the scale of an oyster farm. Front. Mar. Sci. 4, 137. https://doi.org/10.3389/fmars.2017.00137.

Giacobbe, M.G., Oliva, F.D., Maimone, G., 1996. Environmental factors and seasonal occurrence of the dinoflagellate *Alexandrium minutum*, a PSP potential producer, in a mediterranean Lagoon. Estuar. Coast Shelf Sci. 42, 539–549. https://doi.org/10.1006/ecss.1996.0035.

Gilerson, A.A., Gitelson, A.A., Zhou, J., Gurlin, D., Moses, W., Ioannou, I., Ahmed, S.A., 2010. Algorithms for remote estimation of chlorophyll-a in coastal and inland waters using red and near infrared bands. Opt Express 18 (23), 24109–24125. https://doi.org/10.1364/OE.18.024109.

Gitelson, A., 1992. The peak near 700 nm on radiance spectra of algae and water: relationships of its magnitude and position with chlorophyll concentration. Int. J. Rem. Sens. 13, 3367–3373. https://doi.org/10.1080/01431169208904125.

Glibert, P.M., Wilkerson, F.P., Dugdale, R.C., Raven, J.A., Dupont, C.L., Leavitt, P.R., Parker, A.E., Burkholder, J.M., Kana, T.M., 2016. Pluses and minuses of ammonium and nitrate uptake and assimilation by phytoplankton and implications for productivity and community composition, with emphasis on nitrogen-enriched conditions. Limnol. Oceanogr. 61 (1), 165–197. https://doi.org/10.1002/lno.10203.

Gobler, C.J., Doherty, O.M., Hattenrath-Lehmann, T.K., Griffith, A.W., Kang, Y., Litaker, R.W., 2017. Ocean warming since 1982 has expanded the niche of toxic algal blooms in the North Atlantic and North Pacific oceans. Proc. Natl. Acad. Sci. USA 114 (19), 4975–4980. https://doi.org/10.1073/pnas.1619575114.

Hall, N.S., Paerl, H.W., Peierls, B.L., Whipple, A.C., Rossignol, K.L., 2013. Effects of climatic variability on phytoplankton community structure and bloom development in the eutrophic, microtidal, New River Estuary, North Carolina, USA. Estuar. Coast Shelf Sci. 117, 70–82. https://doi.org/10.1016/j.ecss.2012.10.004.

Hallegraeff, G., 2010. Ocean climate change, phytoplankton community responses, and harmful algal blooms: a formidable predictive challenge. J. Phycol. 46, 220–235. https://doi.org/10.1111/j.1529-8817.2010.00815.x.

Hansen, G., Moestrup, Ø., 2005. Flagellar apparatus and nuclear chambers of the green dinoflagellate *Gymnodinium chlorophorum*. Phycol. Res. 53 (2), 169–181. https://doi.org/10.1111/j.1440-183.2005.00383.x.

Hansen, G., Botes, L., De Salas, M., 2007. Ultrastructure and large subunit rDNA sequences of *Lepidodinium viride* reveal a close relationship to *Lepidodinium*

chlorophorum comb. nov. (= *Gymnodinium chlorophorum*). Phycol. Res. 55, 25–41. https://doi.org/10.1111/j.1440-1835.2006.00442.x.

Harmel, T., Chami, M., Tormos, T., Reynaud, N., Danis, P.A., 2018. Sunglint correction of the Multi-Spectral Instrument (MSI)-SENTINEL-2 imagery over inland and sea waters from SWIR bands. Remote Sens. Environ. 204, 308–321. https://doi.org/10.1016/j.rse.2017.10.022.

Hasui, M., Matsuda, M., Okutani, K., Shigeta, S., 1995. *In vitro* antiviral activities of sulfated polysaccharides from a marine microalga (*Cochlodinium polykrikoides*) against human immunodeficiency virus and other enveloped viruses. Int. J. Biol. Macromol. 17, 293–297. https://doi.org/10.1016/0141-8130(95)98157-T.

Herreid, C.F., 1980. Hypoxia in invertebrates. Comp. Biochem. Physiol. 67, 311–320. https://doi.org/10.1016/S0300-9629(80)80002-8.

Hicks, D.W., McMahon, R.F., 2002. Respiratory responses to temperature and hypoxia in the nonindigenous Brown Mussel, *Perna perna* (Bivalvia: mytilidae), from the Gulf of Mexico. J. Exp. Mar. Biol. Ecol. 277, 61–78. https://doi.org/10.1016/S0022-0981(02)00276-9.

Honsell, G., Talarico, L., 2004. *Gymnodinium chlorophorum* (dinophyceae) in the adriatic sea: electron microscopical observations. Bot. Mar. 47, 152–166. https://doi.org/10.1515/BOT.2004.016.

Honsell, G., Talarico, L., Cabrini, M., 1988. Interesting ultrastructural features of a green dinoflagellate. G. Bot. Ital. 122, 76–78.

Iriarte, J.L., Quiñones, R.A., González, R.R., 2005. Relationship between biomass and enzymatic activity of a bloom-forming dinoflagellate (Dinophyceae) in southern Chile (41° S): a field approach. J. Plankton Res. 27 (2), 159–166. https://doi.org/10.1093/plankt/fbh167.

Iverson, R.L., Curl, H.C., O'Connors, H.B., Kirk, J.D., Zakar, K., 1974. Summer phytoplankton blooms in Auke Bay, Alaska, driven by wind mixing of the water column. Limnol. Oceanogr. 19 (2), 271–278. https://doi.org/10.4319/lo.1974.19.2.0271.

Jackson, C., Knoll, A.H., Chan, C.X., Verbruggen, H., 2018. Plastid phylogenomics with broad taxon sampling further elucidates the distinct evolutionary origins and timing of secondary green plastids. Sci. Rep. 8, 1523. https://doi.org/10.1038/s41598-017-18805-w.

Jeong, H.J., Yoo, Y.D., Kang, N.S., Rho, J.R., Seong, K.A., Park, J.W., Nam, G.S., Yih, W., 2010. Ecology of *Gymnodinium aureolum*. I. Feeding in western Korean waters. Aquat. Microb. Ecol. 59, 239–255. https://doi.org/10.3354/ame01394.

Kamikawa, R., Tanifuji, G., Kawachi, M., Miyashita, H., Hashimoto, T., Inagaki, Y., 2015. Plastid genome-based phylogeny pinpointed the origin of the green-colored plastid in the dinoflagellate *Lepidinium chlorophorum*. Genome Biol. Evol. 7 (4), 1133–1140. https://doi.org/10.1093/gbe/evv060.

Karasiewicz, S., Chapelle, A., Bacher, C., Soudant, D., 2020. Harmful algae niche responses to environmental and community variation along the French coast. Harmful Algae 93, 101785. https://doi.org/10.1016/j.hal.2020.101785.

Kononen, K., Huttunen, M., Hällfors, S., Gentien, P., Lunven, M., Huttula, T., Laanemets, J., Lilover, M., Pavelson, J., Stips, A., 2003. Development of a deep chlorophyll maximum of *Heterocapsa triquetra* Ehrenb. at the entrance to the Gulf of Finland. Limnol. Oceanogr. 48 (2), 594–607. https://doi.org/10.4319/lo.2003.48.2.0594.

Lavigne, H., Van der Zande, D., Ruddick, K., Dos Santos, J.C., Gohin, F., Brotas, V., Kratzer, S., 2021. Quality-control tests for OC4, OC5 and NIR-red satellite chlorophyll-a algorithms applied to coastal waters. Remote Sens. Environ. 255, 112237 https://doi.org/10.1016/j.rse.2020.112237.

Lazure, P., Jégou, A.M., 1998. 3D modelling of seasonal evolution of Loire and Gironde plumes on Biscay Bay continental shelf. Oceanol. Acta 21 (2), 165–177. https://doi.org/10.1016/S0399-1784(98)80006-6.

Lazure, P., Salomon, J.C., 1991. Coupled 2-D and 3-D modelling of coastal hydrodynamics. Oceanol. Acta 14 (2), 173–180.

Lazure, P., Garnier, V., Dumas, F., Herry, C., Chifflet, M., 2009. Development of a hydrodynamic model of the Bay of Biscay. Validation of hydrology. Continent. Shelf Res. 29, 985–997. https://doi.org/10.1016/j.csr.2008.12.017.

Lee, Z.P., Du, K.P., Arnone, R., 2005. A model for the diffuse attenuation coefficient of downwelling irradiance. J. Geophys. Res. Oceans 110 (C2) https://doi.org/10.1029/2004JC002275.

Lips, U., Lips, I., Liblik, T., Kuvaldina, N., 2010. Processes responsible for the formation and maintenance of sub-surface chlorophyll maxima in the Gulf of Finland. Estuar. Coast Shelf Sci. 88, 339–349. https://doi.org/10.1016/j.ecss.2010.04.015.

Liu, K., Ng, H.Y.T., Zhang, S., Liu, H., 2021. Effects of temperature on a mixotrophic dinoflagellate (*Lepidinium* sp.) under different nutritional strategies. Mar. Ecol. Prog. Ser. 678, 37–49. https://doi.org/10.3354/meps13865.

Lucas, L.V., Koseff, J.R., Monismith, S.G., Cloern, J.E., Thompson, J.K., 1999a. Processes governing phytoplankton blooms in estuaries. II: the role of horizontal transport. Mar. Ecol. Prog. Ser. 187, 17–30.

Lucas, L.V., Koseff, J.R., Cloern, J.E., Monismith, S.G., Thompson, J.K., 1999b. Processes governing phytoplankton blooms in estuaries. I: the local production-loss balance. Mar. Ecol. Prog. Ser. 187, 1–15.

Lyons, M.M., Lau, Y.T., Carden, W.E., Ward, J.E., Roberts, S.B., Smolowitz, R., Vallino, J., Allam, B., 2007. Characteristics of marine aggregates in shallow-water ecosystems: implications for disease ecology. EcoHealth 4 (4), 406–420. https://doi.org/10.1007/s10393-007-0134-0.

Main-Knorn, M., Pflug, B., Louis, J., Debaecker, V., Müller-Wilm, U., Gascon, F., 2017. Sen2Cor for Sentinel-2. SPIE Remote Sensing, vol. 12. SPIE. https://doi.org/10.1117/12.2278218.

Mandal, S.K., Singh, R.P., Patel, V., 2011. Isolation and characterization of exopolysaccharide secreted by a toxic dinoflagellate, *Amphidinium carterae* hulburt 1957 and its probable role in harmful algal blooms (HABs). Microb. Ecol. 62, 518–527. https://doi.org/10.1007/s00248-011-9852-5.

Margalef, R., 1978. Life-forms of phytoplankton as survival alternatives in an unstable environment. Oceanol. Acta 1 (4), 493–509.

Mari, X., Passow, U., Migon, C., Burd, A.B., Legendre, L., 2017. Transparent exopolymer particles: effects on carbon cycling in the ocean. Prog. Oceanogr. 151, 13–37. https://doi.org/10.1016/j.pocean.2016.11.002.

Matsumoto, T., Shinozaki, F., Chikuni, T., Yabuki, A., Takishita, K., Kawachi, M., Nakayama, T., Inouye, I., Hashimoto, T., Inagaki, Y., 2011. Green-colored plastids in the dinoflagellate genus *Lepidinium* are of Core chlorophyte origin. Protist 162, 268–276. https://doi.org/10.1016/j.protis.2010.07.001.

McCarthy, P.M., 2013. Census of Australian Marine Dinoflagellates. Australian Biological Resources Study. Canberra. http://www.anbg.gov.au/abrs/Dinoflagellates/index_Dino.html. version.

Ménesguen, A., Dussauze, M., 2015. Détermination des "bassins récepteurs" marins des principaux fleuves français de la façade Manche-Atlantique, et de leurs rôles respectifs dans l'eutrophisation phytoplanctonique des masses d'eau DCE et des sous-régions DCSMM. Nantes, France. https://archimer.ifremer.fr/doc/00333/44422/.

Ménesguen, A., Desmit, X., Dulière, V., Lacroix, G., Thouvenin, B., Thieu, V., Dussauze, M., 2018. How to avoid eutrophication in coastal seas? A new approach to derive river-specific combined nitrate and phosphate maximum concentrations. Sci. Total Environ. 628–629, 400–414. https://doi.org/10.1016/j.scitotenv.2018.02.025.

Ng, W.H.A., Liu, H., Zhang, S., 2017. Diel variation of grazing of the dinoflagellate *Lepidinium* sp. and ciliate Euplotes sp. on algal prey: the effect of prey cell properties. J. Plankton Res. 39 (3), 450–462. https://doi.org/10.1093/plankt/fbx020.

Nielsen, T.G., Kiørboe, T., Bjørnsen, P.K., 1990. Effects of a *Chrysochromulina polylepis* subsurface bloom on the planktonic community. Mar. Ecol. Prog. Ser. 62 (1/2), 21–35. https://doi.org/10.3354/meps062021.

Odebrecht, C., Abreu, P.C., Carstensen, J., 2015. Retention time generates short-term phytoplankton blooms in a shallow microtidal subtropical estuary. Estuar. Coast Shelf Sci. 162, 35–44. https://doi.org/10.1016/j.ecss.2015.03.004.

Ortega-Retuerta, E., Reche, I., Pulido-Villena, E., Agustí, S., Duarte, C.M., 2009. Uncoupled distributions of transparent exopolymer particles (TEP) and dissolved carbohydrates in the Southern Ocean. Mar. Chem. 115, 59–65. https://doi.org/10.1016/j.marchem.2009.06.004.

Ortega-Retuerta, E., Duarte, C.M., Reche, I., 2010. Significance of bacterial activity for the distribution and dynamics of transparent exopolymer particles in the Mediterranean Sea. Microb. Ecol. 59, 808–818. https://doi.org/10.1007/s00248-010-9640-7.

O'Reilly, J.E., Maritorena, S., Mitchell, B.G., Siegel, D.A., Carder, K.L., Garver, S.A., Kahru, M., McClain, C., 1998. Ocean color chlorophyll algorithm for SeaWiFS. J. Geophys. Res. 103, 24937–24953.

Paerl, H.W., 1997. Coastal eutrophication and harmful algal blooms: importance of atmospheric deposition and groundwater as "new" nitrogen and other nutrient sources. Limnol. Oceanogr. 42 (5), 1154–1165. https://doi.org/10.4319/lo.1997.42.5_part_2.1154.

Passow, U., 2002. Transparent exopolymer particles (TEP) in aquatic environments. Prog. Oceanogr. 55, 287–333. https://doi.org/10.1016/S0079-6611(02)00138-6.

Passow, U., Alldredge, A.L., 1995. A dye-binding assay for the spectrophotometric measurement of transparent exopolymer particles (TEP). Limnol. Oceanogr. 40 (7), 1326–1335. https://doi.org/10.4319/lo.1995.40.7.1326.

Passow, U., Engel, A., 2001. Carbon and nitrogen content of transparent exopolymer particles (TEP) in relation to their Alcian Blue adsorption. Mar. Ecol. Prog. Ser. 219, 1–10. https://doi.org/10.3354/meps219001.

Passow, U., Shipe, R.F., Murray, A., Pak, D.K., Brzezinski, M.A., Alldredge, A.L., 2001. The origin of transparent exopolymer particles (TEP) and their role in the sedimentation of particulate matter. Continent. Shelf Res. 21, 327–346.

Paulmier, G., Berland, B., Billard, C., Nezan, E., 1995. *Gyrodinium corsicum* nov. sp. (Gymnodiniales, Dinophycees), organisme responsable d'une «eau Verte» dans l'Etang marin de Diana (Corse), en Avril 1994. Cryptogam. Algol. 16, 77–94.

Peierls, B.L., Hall, N.S., Paerl, H.W., 2012. Non-monotonic responses of phytoplankton biomass accumulation to hydrologic variability: a comparison of two coastal plain North Carolina Estuaries. Estuar. Coast 35, 1376–1392. https://doi.org/10.1007/s12237-012-9547-2.

Petersen, J.K., Nielsen, T.G., van Duren, L., Maar, M., 2008. Depletion of plankton in a raft culture of *Mytilus galloprovincialis* in Ría de Vigo, NW Spain. I. Phytoplankton. Aquat. Biol. 4, 113–125. https://doi.org/10.3354/ab00124.

Planque, B., Lazure, P., Jégou, A.M., 2004. Detecting hydrological landscapes over the Bay of Biscay continental shelf in spring. Clim. Res. 28, 41–52. https://doi.org/10.3354/cr028041.

Prieto, L., Navarro, G., Cózar, A., Echevarría, F., García, C.M., 2006. Distribution of TEP in the euphotic and upper mesopelagic zones of the southern Iberian coasts. Deep Sea Res. II 53, 1314–1328. https://doi.org/10.1016/j.dsr2.2006.03.009.

Puillat, I., Lazure, P., Jégou, A.M., Lampert, L., Miller, P., 2004. Hydrographical variability on the French continental shelf in the Bay of Biscay, during the 1990s. Continent. Shelf Res. 24, 1143–1163. https://doi.org/10.1016/j.csr.2004.02.008.

Puillat, I., Lazure, P., Jégou, A.M., Lampert, L., Miller, P., 2006. Mesoscale Hydrological Variability Induced by Northwesterly Wind on the French Continental Shelf of the Bay of Biscay. Scientia Marina, pp. 15–26. https://doi.org/10.3989/scimar.2006.70s115.

Qi, L., Hu, C., 2021. To what extent can *Ulva* and *Sargassum* be detected and separated in satellite imagery? Harmful Algae 103, 102001. https://doi.org/10.1016/j.hal.2021.102001.

Quevedo, M., Gonzalez-Quiros, R., Anadon, R., 1999. Evidence of heavy predation by *Noctiluca scintillans* on *Acartia clausi* (Copepoda) eggs off the central Cantabrian coast

(NW Spain). Oceanol. Acta 22 (1), 127–131. https://doi.org/10.1016/S0399-1784 (99)80039-5.

Raimbault, P., Pouvesle, W., Diaz, F., Garcia, N., Sempere, R., 1999. Wet-oxidation and automated colorimetry for simultaneous determination of organic carbon, nitrogen and phosphorus dissolved in seawater. Mar. Chem. 66, 161–169. https://doi.org/10.1016/S0304-4203(99)00038-9.

Ratmaya, W., Soudant, D., Salmon-Monviola, J., Plus, M., Cochennec-Laureau, N., Goubert, E., Andrieux-Loyer, F., Barillé, L., Souchu, P., 2019. Reduced phosphorus loads from the Loire and Vilaine rivers were accompanied by increasing eutrophication in the Vilaine Bay (south Brittany, France). Biogeosciences 16, 1361–1380. https://doi.org/10.5194/bg-16-1361-2019.

Redfield, A.C., 1958. The biological control of chemical factors in the environment. Am. Sci. 46 (3), 205–221. https://www.jstor.org/stable/27827150.

Retho, M., Quemener, L., Le Gall, C., Repecaud, M., Souchu, P., Gabellec, R., Manach, S., 2020. MOLIT Vilaine Data and Metadata from Coriolis Data Centre. SEANOE. https://doi.org/10.17882/46529.

Richardson, K., Visser, A.W., Pedersen, F.B., 2000. Subsurface phytoplankton blooms fuel pelagic production in the North Sea. J. Plankton Res. 22 (9), 1663–1671. https://doi.org/10.1093/plankt/22.9.1663.

Rodríguez-Benito, C.V., Navarro, G., Caballero, I., 2020. Using Copernicus Sentinel-2 and Sentinel-3 data to monitor harmful algal blooms in Southern Chile during the COVID-19 lockdown. Mar. Pollut. Bull. 161, 111722 https://doi.org/10.1016/j.marpolbul.2020.111722.

Rosenberg, R., Hellman, B., Johansson, B., 1991. Hypoxic tolerance of marine benthic fauna. Mar. Ecol. Prog. Ser. 79, 127–131. https://doi.org/10.3354/meps079127.

Rossignol-Strick, M., 1985. A marine anoxic event on the Brittany coast, July 1982. J. Coast Res. 1 (1), 11–20.

Roux, P., Siano, R., Collin, K., Bilien, G., Sinquin, C., Marchand, L., Zykwinska, A., Delbarre-Ladrat, C., Schapira, M., 2021. Bacteria enhance the production of extracellular polymeric substances by the green dinoflagellate *Lepidodinium chlorophorum*. Sci. Rep. 11, 4795. https://doi.org/10.1038/s41598-021-84253-2.

Schapira, M., McQuaid, C.D., Froneman, P.W., 2012a. Metabolism of free-living and particle-associated prokaryotes: consequences for carbon flux around a Southern Ocean archipelago. J. Mar. Syst. 90, 58–66. https://doi.org/10.1016/j.jmarsys.2011.08.009.

Schapira, M., McQuaid, C.D., Froneman, P.W., 2012b. Free-living and particle-associated prokaryote metabolism in giant kelp forests: implications for carbon flux in a sub-Antarctic coastal area. Estuar. Coast Shelf Sci. 106, 69–79. https://doi.org/10.1016/j.ecss.2012.04.031.

Schlitzer, R., 2020. Ocean Data View. http://odv.awi.de.

Serre-Fredj, L., Jacqueline, F., Navon, M., Izabel, G., Chasselin, L., Jolly, O., Repecaud, M., Claquin, P., 2021. Coupling high frequency monitoring and bioassay experiments to investigate a harmful algal bloom in the Bay of Seine (French-English Channel). Mar. Pollut. Bull. 168, 112387 https://doi.org/10.1016/j.marpolbul.2021.112387.

Shapiro, K., Krusor, C., Mazzillo, F.F.M., Conrad, P.A., Largier, J.L., Mazet, J.A.K., Silver, M.W., 2014. Aquatic polymers can drive pathogen transmission in coastal ecosystems. Proc. Royal Soc. B 281 (1795), 1–9. https://doi.org/10.1098/rspb.2014.1287.

Shikata, T., Nagasoe, S., Matsubara, T., Yoshikawa, S., Yamasaki, Y., Shimasaki, Y., Oshima, Y., Jenkinson, I.R., Honjo, T., 2008. Factors influencing the initiation of blooms of the raphidophyte *Heterosigma akashiwo* and the diatom *Skeletonema costatum* in a port in Japan. Limnol. Oceanogr. 53 (6), 2503–2518. https://doi.org/10.2307/40058340.

Siano, R., Alves-De-Souza, C., Foulon, E., Bendif, E.M., Simon, N., Guillou, L., Not, F., 2011. Distribution and host diversity of Amoebophryidae parasites across oligotrophic waters of the Mediterranean Sea. Biogeosciences 8, 267–278. https://doi.org/10.5194/bg-8-267-2011.

Siano, R., Chapelle, A., Antoine, V., Michel-Guillou, E., Rigaut-Jalabert, F., Guillou, L., Hégaret, H., Leynaert, A., Curd, A., 2020. Citizen participation in monitoring phytoplankton seawater discolorations. Mar. Pol. 117, 103039 https://doi.org/10.1016/j.marpol.2018.01.022.

Simon, M., Grossart, H.P., Schweitzer, B., Ploug, H., 2002. Microbial ecology of organic aggregates in aquatic ecosystems. Aquat. Microb. Ecol. 28 (2), 175–211. https://doi.org/10.3354/ame028175.

Smayda, T.J., 2002a. Turbulence, watermass stratification and harmful algal blooms: an alternative view and frontal zones as "pelagic seed banks. Harmful Algae 1, 95–112. https://doi.org/10.1016/S1568-9883(02)00010-0.

Smayda, T.J., 2002b. Adaptive ecology, growth strategies and the global bloom expansion of dinoflagellates. J. Oceanogr. 58, 281–294. https://doi.org/10.1023/A:1015861725470.

Sobral, P., Widdows, J., 1997. Influence of hypoxia and anoxia on the physiological responses of the clam *Ruditapes decussatus* from southern Portugal. Mar. Biol. 127, 455–461. https://doi.org/10.1007/s002270050033.

Sourisseau, M., Jegou, K., Lunven, M., Quere, J., Gohin, F., Bryere, P., 2016. Distribution and dynamics of two species of Dinophyceae producing high biomass blooms over the French Atlantic Shelf. Harmful Algae 53, 53–63. https://doi.org/10.1016/j.hal.2015.11.016.

Sournia, A., Belin, C., Billard, C., Erard-Le Denn, E., Fresnel, J., Lassus, P., Pastoureau, A., Soulard, R., 1992. The repetitive and expanding occurrence of green, bloom-forming dinoflagellate (Dinophyceae) on the coasts of France. Cryptogam. Algol. 13 (1), 1–13.

Steinmetz, F., Deschamps, P.Y., Ramon, D., 2011. Atmospheric correction in presence of sun glint: application to MERIS. Opt Express 19 (10), 9783–9800. https://doi.org/10.1364/OE.19.009783.

Suttle, C.A., 2007. Marine viruses - major players in the global ecosystem. Nat. Rev. Microbiol. 5, 801–812. https://doi.org/10.1038/nrmicro1750.

Thomas, Y., Pouvreau, S., Alunno-Bruscia, M., Barillé, L., Gohin, F., Bryere, P., Gernez, P., 2016. Global change and climate-driven invasion of the Pacific oyster (*Crassostrea gigas*) along European coasts: a bioenergetics modelling approach. J. Biogeogr. 43 (3), 568–579. https://doi.org/10.1111/jbi.12665.

Traini, C., Proust, J.N., Menier, D., Mathew, M.J., 2015. Distinguishing natural evolution and human impact on estuarine morpho-sedimentary development: a case study from the Vilaine Estuary. France. Estuar. Coast. Shelf Sci. 163, 143–155. https://doi.org/10.1016/j.ecss.2015.06.025.

Utermöhl, H., 1958. Zur vervollkommnung der quantitativen phytoplankton methodik. Mitteilungen-Internationale Vereiningung fur Limnologie. 9, 1–38.

Velo-Suárez, L., Reguera, B., Garcés, E., Wyatt, T., 2009. Vertical distribution of division rates in coastal dinoflagellate *Dinophysis* spp. populations: implications for modelling. Mar. Ecol. Prog. Ser. 385, 87–96. https://doi.org/10.3354/meps08014.

Yamamoto, K., Tsujimura, H., Nakajima, M., Harrison, P.J., 2013. Flushing rate and salinity may control the blooms of the toxic dinoflagellate *Alexandrium tamarense* in a river/estuary in Osaka Bay, Japan. J. Oceanogr. 69, 727–736. https://doi.org/10.1007/s10872-013-0203-7.

Yim, J.H., Kim, S.J., Ahn, S.H., Lee, H.K., 2007. Characterization of a novel bioflocculant, p-KG03, from a marine dinoflagellate, *Gyrodinium impudicum* KG03. Bioresour. Technol. 98 (2), 361–367. https://doi.org/10.1016/j.biortech.2005.12.021.

Zeng, C., Binding, C., 2019. The effect of mineral sediments on satellite chlorophyll-a retrievals from line-height algorithms using red and near-infrared bands. Rem. Sens. 11 (19), 2306. https://doi.org/10.3390/rs11192306.

Zhang, W., Dong, Z., Zhang, C., Sun, X., Hou, C., Liu, Y., Wang, L., Ma, Y., Zhao, J., 2020. Effects of physical-biochemical coupling processes on the *Noctiluca scintillans* and *Mesodinium* red tides in October 2019 in the Yantai nearshore, China. Mar. Pollut. Bull. 160, 111609 https://doi.org/10.1016/j.marpolbul.2020.111609.

Zingone, A., Enevoldsen, O.H., 2000. The diversity of harmful algal blooms: a challenge for science and management. Ocean Coast Manag. 43, 725–748. https://doi.org/10.1016/S0964-5691(00)00056-9.

Further reading

REPHY, 2021. French observation and monitoring program for phytoplankton and hydrology in coastal waters. In: REPHY Dataset - French Observation and Monitoring Program for Phytoplankton and Hydrology in Coastal Waters. Metropolitan data. SEANOE. https://doi.org/10.17882/47248.